CONFIDENTIAL

NACA RM L53F09

NACA

RESEARCH MEMORANDUM

WIND-TUNNEL INVESTIGATION OF THE EFFECTS OF GEOMETRIC DIHEDRAL ON THE AERODYNAMIC CHARACTERISTICS IN PITCH AND SIDESLIP OF AN UNSWEPT- AND A 45° SWEPTBACK-WING-FUSELAGE COMBINATION AT HIGH SUBSONIC SPEEDS

By Richard E. Kuhn and John W. Draper

Langley Aeronautical Laboratory
Langley Field, Va.

NATIONAL ADVISORY COMMITTEE
FOR AERONAUTICS

WASHINGTON
July 29, 1953

CONFIDENTIAL

NATIONAL ADVISORY COMMITTEE FOR AERONAUTICS

RESEARCH MEMORANDUM

WIND-TUNNEL INVESTIGATION OF THE EFFECTS OF GEOMETRIC DIHEDRAL ON THE AERODYNAMIC CHARACTERISTICS IN PITCH AND SIDESLIP OF AN UNSWEPT- AND A 45° SWEPTBACK-WING–FUSELAGE COMBINATION AT HIGH SUBSONIC SPEEDS

By Richard E. Kuhn and John W. Draper

SUMMARY

An investigation was made in the Langley high-speed 7- by 10-foot tunnel to determine the effects of geometric dihedral on the aerodynamic characteristics of wing-fuselage combinations having wings of aspect ratio 4, taper ratio 0.6, and angles of sweep of 3.6° and 45° at the quarter-chord line. The investigation covered dihedral angles of -10°, -5°, 5°, and 10° and a Mach number range from 0.40 to 0.95. In order to expedite publication only a very brief analysis has been included; however, the results indicate that at angles of attack to about 6° the effect of geometric dihedral on the effective-dihedral parameter is slightly larger than would be predicted. At angles of attack corresponding roughly to the stall, the effect of geometric dihedral on the effective-dihedral parameter was rather small and somewhat erratic.

INTRODUCTION

A systematic research program is being conducted in the Langley high-speed 7- by 10-foot tunnel to determine the aerodynamic characteristics in pitch and sideslip of a series of wing plan forms at high subsonic speeds. (For example, see refs. 1 and 2.) The configurations investigated are wing-fuselage combinations with the wing mounted in the midwing position at zero dihedral. Some data on the effects of geometric dihedral on the low-speed characteristics of a 45° swept wing are given in reference 3 and some theoretical predictions of the effects of dihedral are given in reference 4.

This paper presents some data, at Mach numbers up to 0.95, on the effects of geometric dihedral on the aerodynamic characteristics in pitch and sideslip of an unswept and a 45° sweptback wing. The tests covered dihedral angles from -10° to 10° and angles of attack up to 24°. In order to expedite publication, only a very brief analysis of the results is presented.

COEFFICIENTS AND SYMBOLS

The stability system of axes used for the presentation of the data, together with an indication of the positive directions of forces, moments, and angles, is presented in figure 1. All coefficients are based on the area and span of the wing with zero dihedral and the moments for all dihedral configurations are referred to a common moment reference point at the projection of the quarter-chord points of the mean aerodynamic chord on the fuselage center line.

C_L lift coefficient, Lift/qS

C_m pitching-moment coefficient, Pitching moment/qS$\bar{c}$

C_D drag coefficient, Drag/qS

C_l rolling-moment coefficient, Rolling moment/qSb

C_n yawing-moment coefficient, Yawing moment/qSb

C_Y lateral-force coefficient, Lateral-force/qS

q dynamic pressure, $\rho V^2/2$, lb/sq ft

ρ mass density of air, slugs/cu ft

V free-stream velocity, ft/sec

M Mach number

R Reynolds number, $\frac{\rho V \bar{c}}{\mu}$

μ absolute viscosity of air, slugs/ft-sec

S wing area, sq ft

b wing span, ft

c wing chord, ft

$\bar{c}$ mean aerodynamic chord, $\frac{2}{S}\int_0^{b/2} c^2 dy$, ft

α angle of attack, deg

β angle of sideslip, deg

Γ geometric dihedral angle, deg (measured in a plane perpendicular to the plane of symmetry)

Λ sweepback angle of quarter-chord line, deg

$\Delta C_{D_{bp}}$ base-pressure drag coefficient

$C_{l_\beta} = \frac{\partial C_l}{\partial \beta}$, per deg

$C_{n_\beta} = \frac{\partial C_n}{\partial \beta}$, per deg

$C_{Y_\beta} = \frac{\partial C_Y}{\partial \beta}$, per deg

$C_{l_{\beta_\Gamma}} = \frac{\partial C_{l_\beta}}{\partial \Gamma}$, per deg

MODEL AND APPARATUS

The wing-fuselage combinations tested are shown in figure 2 and are two of the wing-fuselage combinations used in the investigations reported in references 1 and 2. Both wings had an NACA 65A006 airfoil section parallel to the fuselage center line and were attached to the fuselage in a midwing position. Shim blocks used to obtain the desired dihedral angle were designed so that the wing-chord plane always intersected the fuselage center line. Negative dihedral angles were obtained by testing the model inverted.

The 3.6° sweptback wing was constructed of solid aluminum alloy. The 45° sweptback wing was of composite construction, consisting of a steel core and a bismuth-tin covering. The ordinates of the aluminum fuselage, which was used for both configurations, are presented in reference 5.

The models were tested on the sting-type support system shown in figures 3 and 4. With this support system the model can be remotely operated through a 28° angle-of-attack range in the plane of the vertical strut. By using couplings in the sting behind the model, the model can be rolled through 90° so that either angle of attack (fig. 3) or angle of sideslip (fig. 4) can be the remotely-controlled variable. With the wings horizontal (fig. 3) the couplings can be used to support the model at angles of sideslip of approximately -4° and 4°, while the model is tested through the angle-of-attack range.

TESTS AND CORRECTIONS

The tests were conducted in the Langley high-speed 7- by 10-foot tunnel. Six component measurements were made by means of an internally mounted strain-gage balance for dihedral angles of -10°, -5°, 5° and 10°. All configurations were tested at angles of sideslip of -4°, 0°, and 4° through an angle-of-attack range from -3° to 24° at several selected Mach numbers. In addition, all configurations were tested at 0° angle of attack through a sideslip-angle range from -3° to 12° at Mach numbers up to 0.95. The estimated choking Mach numbers were 0.94 and 0.96 for the 3.6° and 45° sweptback configurations, respectively. The blocking corrections which were applied were determined by the velocity-ratio method of reference 6.

The variation of Reynolds number with test Mach number is presented in figure 5 and is based on the wing mean aerodynamic chord of 0.765 feet.

The jet-boundary corrections which were applied to the angle of attack and drag were determined from reference 7. The corrections to the other components are negligible. Tare values were determined and were found to be negligible for all components except drag. A drag-coefficient increment of 0.002 should be added to the data presented to account for the interference of the sting. The drag data have been adjusted to correspond to a pressure at the base of the fuselage equal to free-stream static pressure. For this correction, the base pressure was determined by measuring the pressure at a point inside the fuselage 9 inches forward of the base. The correction, which was added to the data and which did not change with dihedral angle, is presented in figure 6.

The angle of attack and angle of sideslip have been corrected for the deflection of the sting-support system and balance under load.

No corrections for the aeroelastic distortion have been applied to the data presented. Although the corrections developed in references 1 and 2 are applicable to the basic data, the effect of aeroelastic distortion on the effects of geometric dihedral would be expected to be small.

PRESENTATION OF RESULTS

The results of the investigation are presented in the following figures:

The data for the zero dihedral configurations (figs. 7 to 12) were taken from references 1 and 2 and are presented again here for completeness and ease of comparison.

A comparison of the effective dihedral parameter $C_{l_{\beta_\Gamma}}$ with available wing-alone theory indicates that the experimental dihedral effect was only slightly larger than that predicted for either of the two wings throughout the test Mach number range. It may be noted from the basic data of figure 10, however, that the values of $C_{l_{\beta_\Gamma}}$ given in figure 17 apply only at angles of attack to about 6°. At higher angles of attack, variations in geometric dihedral have an erratic effect on C_{l_β} and at 20° angle of attack for the unswept wing the highest positive effective

dihedral actually is obtained with the largest negative geometric dihedral. At angles of attack corresponding roughly to the stall, the effect of geometric dihedral on the effective dihedral parameter was rather small.

CONCLUDING REMARKS

An investigation of the effects of geometric dihedral angle on the characteristics in pitch and sideslip of 3.6° and 45° sweptback-wing–fuselage combinations indicates that at angles of attack up to about 6° the effect of geometric dihedral on the effective-dihedral parameter is slightly larger than the predicted effect. At angles of attack corresponding roughly to the stall, the effect of geometric dihedral on the effective-dihedral parameter was rather small and somewhat erratic.

Langley Aeronautical Laboratory,
National Advisory Committee for Aeronautics,
Langley Field, Va., May 25, 1953.

REFERENCES

1. Wiggins, James W., and Kuhn, Richard E.: Wind-Tunnel Investigation of the Aerodynamic Characteristics in Pitch of Wing-Fuselage Combinations at High-Subsonic Speeds. Sweep Series. NACA RM L52D18, 1952.

2. Kuhn, Richard E., and Fournier, Paul G.: Wind-Tunnel Investigation of the Static Lateral Stability Characteristics of Wing-Fuselage Combinations at High Subsonic Speeds - Sweep Series. NACA RM L52G11a, 1952.

3. Queijo, M. J., and Jaquet, Byron M.: Investigation of Effects of Geometric Dihedral on Low-Speed Static Stability and Yawing Characteristics of an Untapered 45° Sweptback-Wing Model of Aspect Ratio 2.61. NACA TN 1668, 1948.

4. Bird, John D.: Some Theoretical Low-Speed Span Loading Characteristics of Swept Wings in Roll and Sideslip. NACA Rep. 969, 1950. (Supersedes NACA TN 1839.)

5. Kuhn, Richard E., and Wiggins, James W.: Wind-Tunnel Investigation of the Aerodynamic Characteristics in Pitch of Wing-Fuselage Combinations at High Subsonic Speeds. Aspect-Ratio Series. NACA RM L52A29, 1952.

6. Hensel, Rudolph W.: Rectangular-Wind-Tunnel Blocking Corrections Using the Velocity-Ratio Method. NACA TN 2372, 1951.

7. Gillis, Clarence L., Polhamus, Edward C., and Gray, Joseph L., Jr.: Charts for Determining Jet-Boundary Corrections for Complete Models in 7- by 10-Foot Closed Rectangular Wind Tunnels. NACA WR L-123, 1945. (Formerly NACA ARR L5G31.)

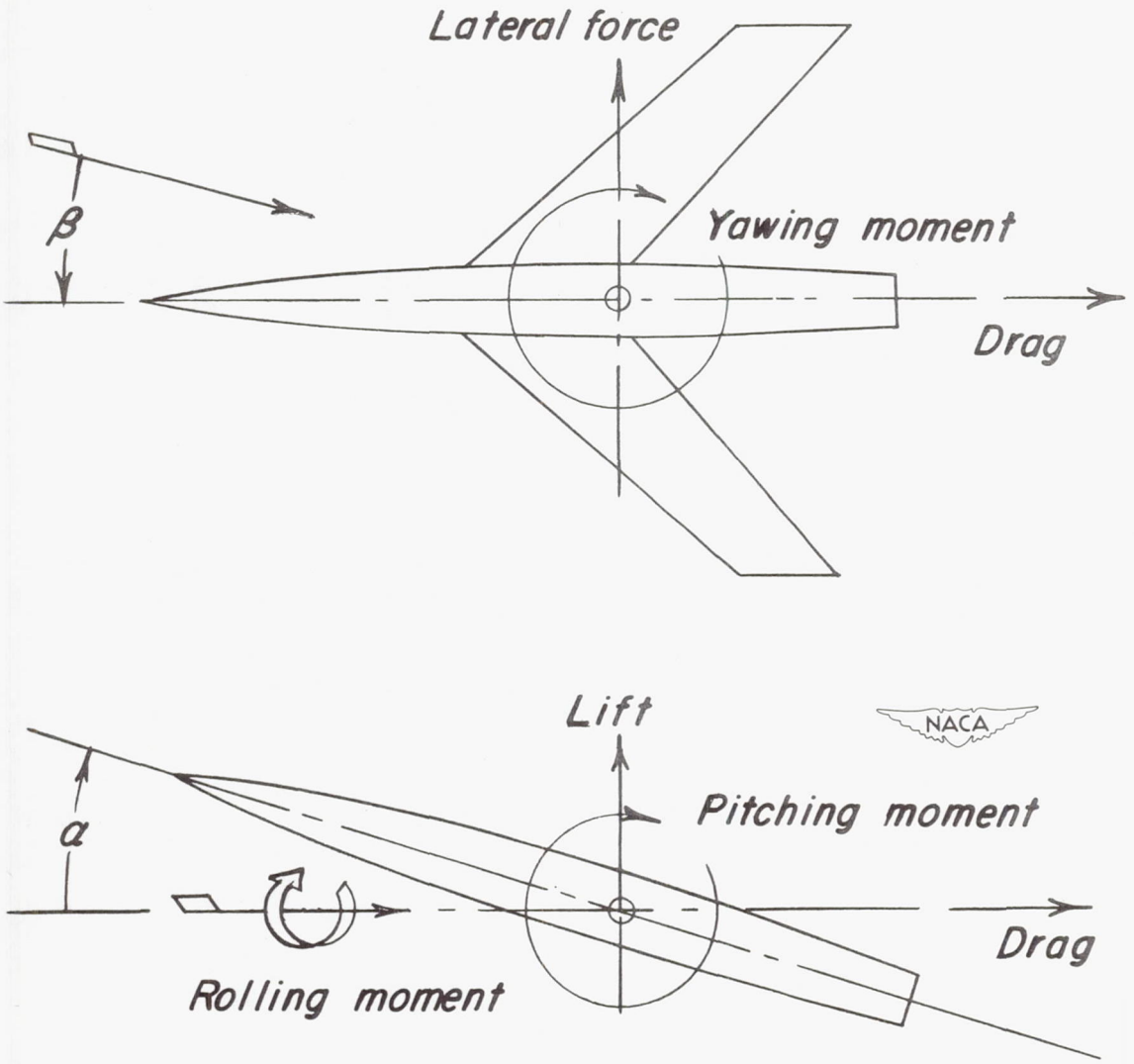

Figure 1.- System of axes used showing positive direction of forces, moments, angles, and velocities.

Fuselage:

Length	4.1 ft
Max. diam.	.416 ft
Position of max. diam.	2.5 ft

Wing:

Area	2.25 sq ft
Span	3.0 ft
Chord	
Tip	.562 ft
Root	.938 ft
Mean aerodynamic chord	.765 ft
Aspect ratio	4
Taper ratio	.6
Incidence	0
Airfoil section parallel to fuselage ℄	NACA 65A006

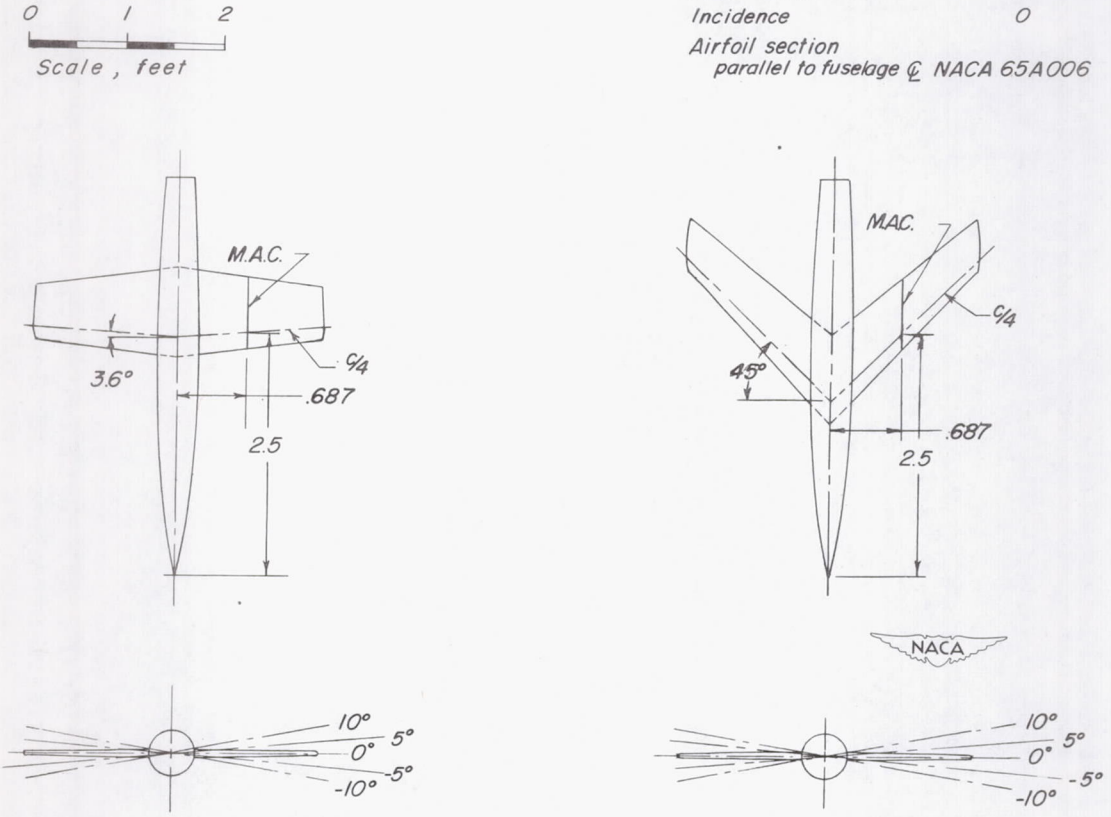

$\Lambda = 3.6°$ $\Lambda = 45°$

Figure 2.- Geometry of the models.

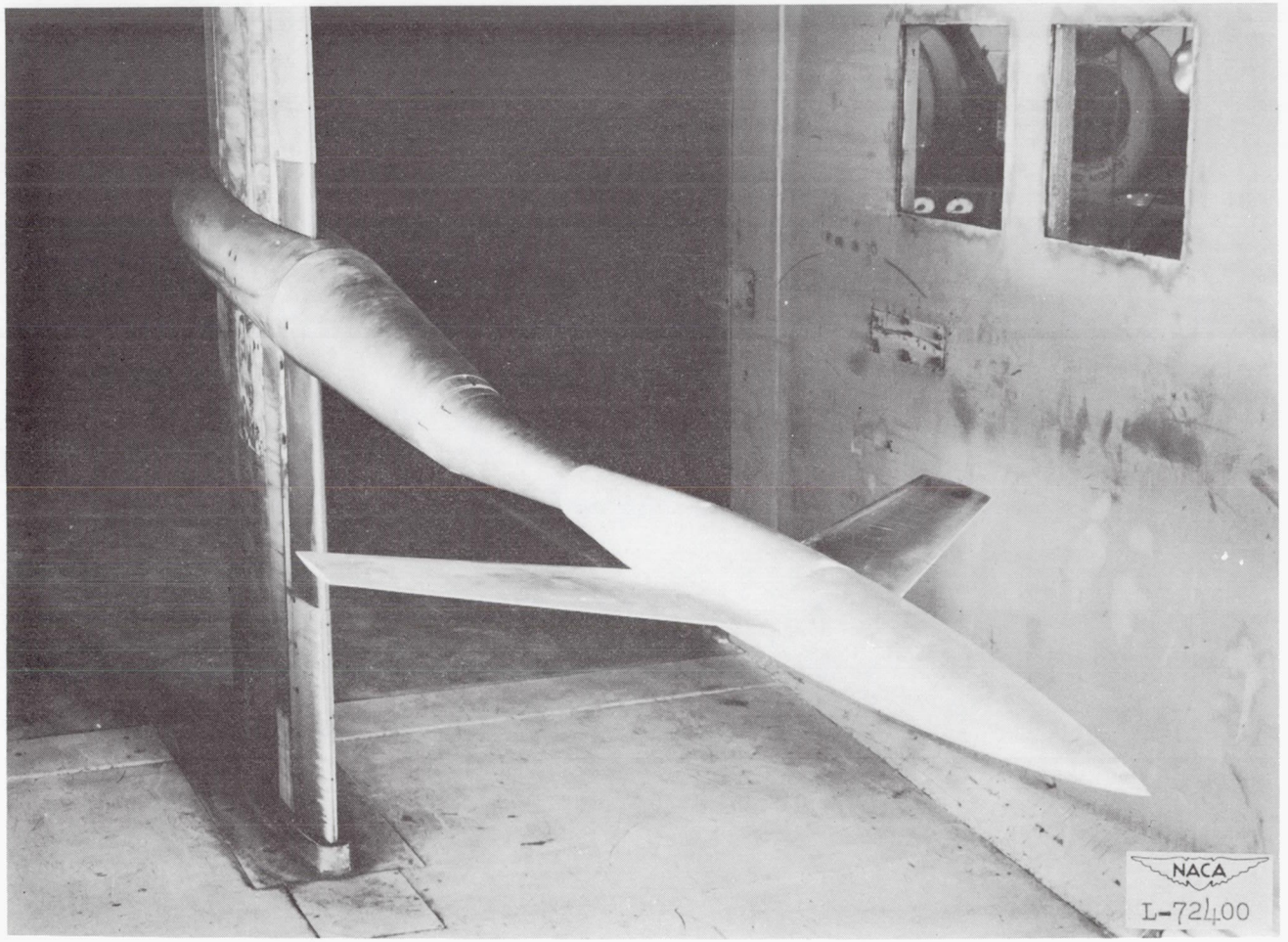

Figure 3.- A typical model installed on the sting support system for variable-angle-of-attack tests. Shown at 4° angle of sideslip.

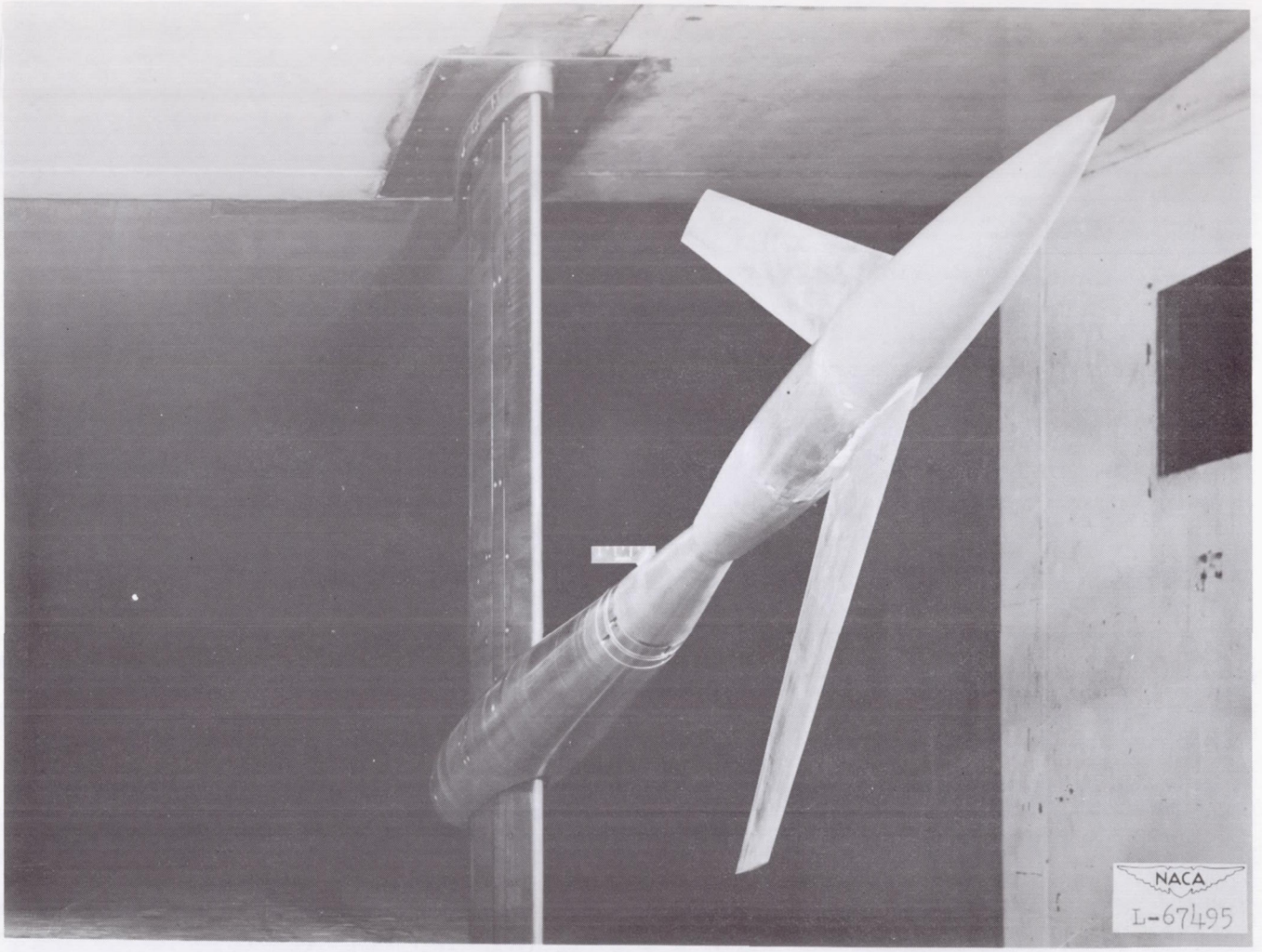

Figure 4.- A typical model installed for variable-angle-of-sideslip tests. Shown at 0° angle of attack.

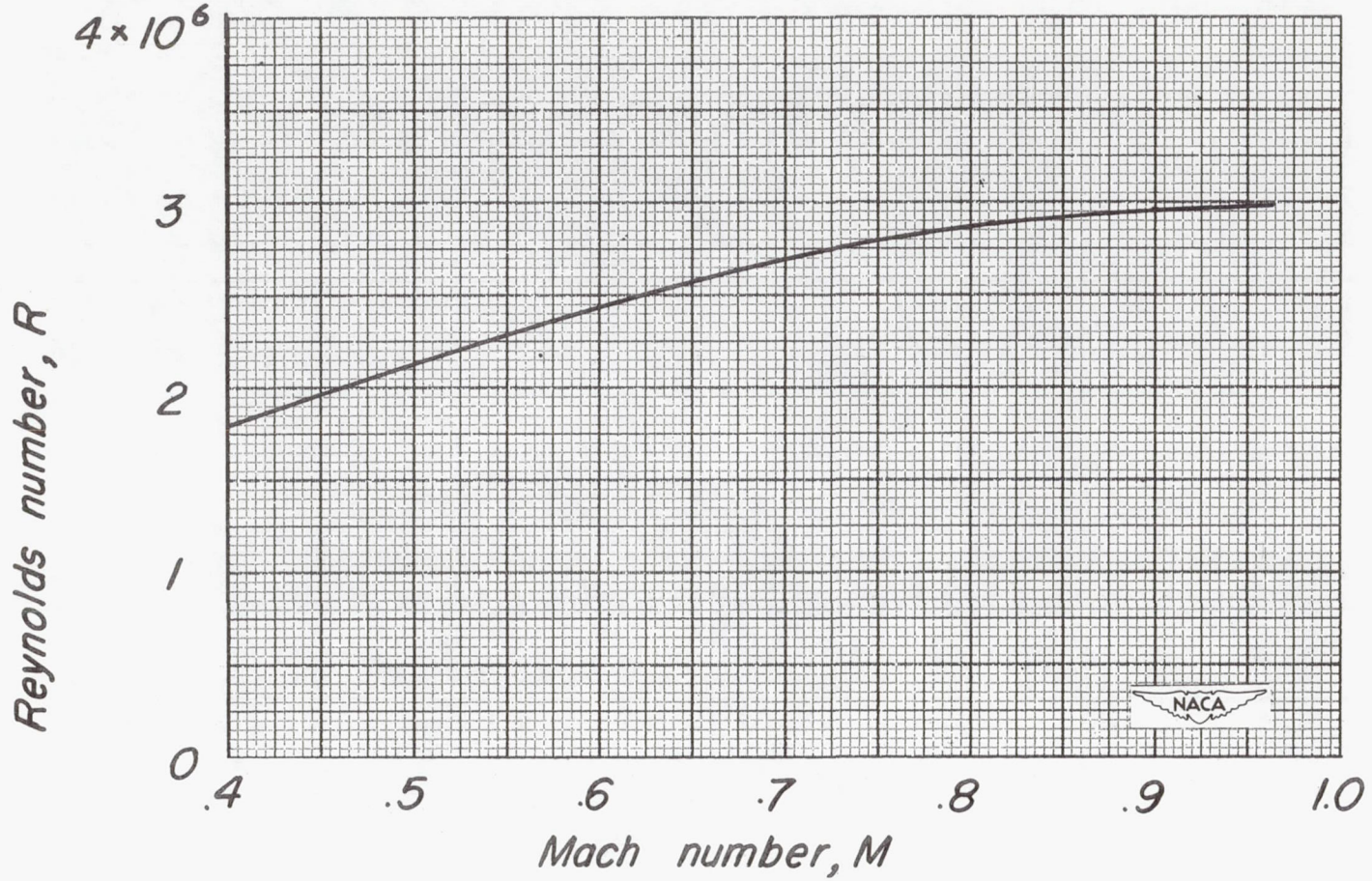

Figure 5.- Variation of Reynolds number with Mach number.

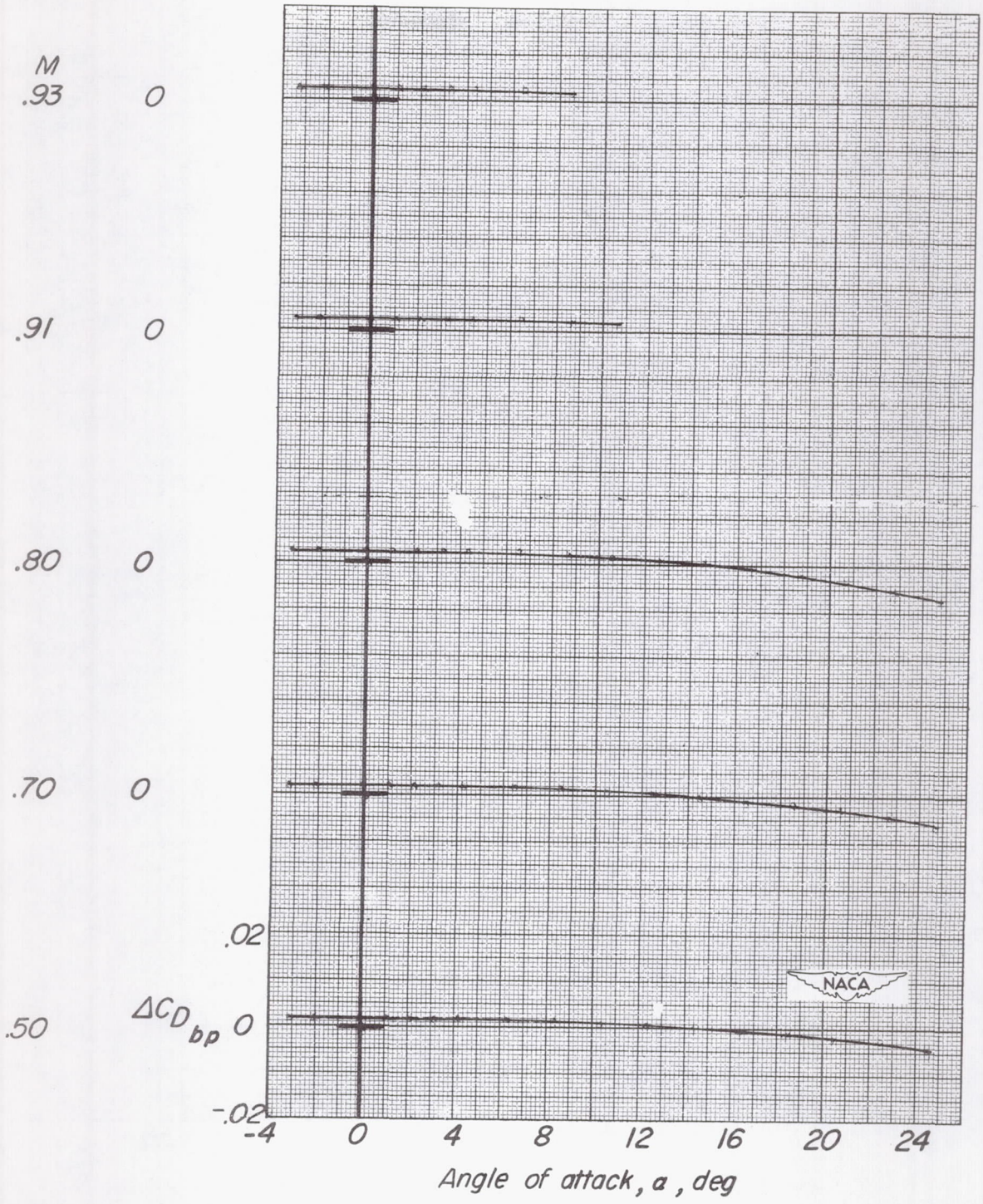

(a) $\Lambda = 3.6^{\circ}$.

Figure 6.- Increment of drag coefficient due to base pressure for all dihedral angles. $\beta = 0^{\circ}$.

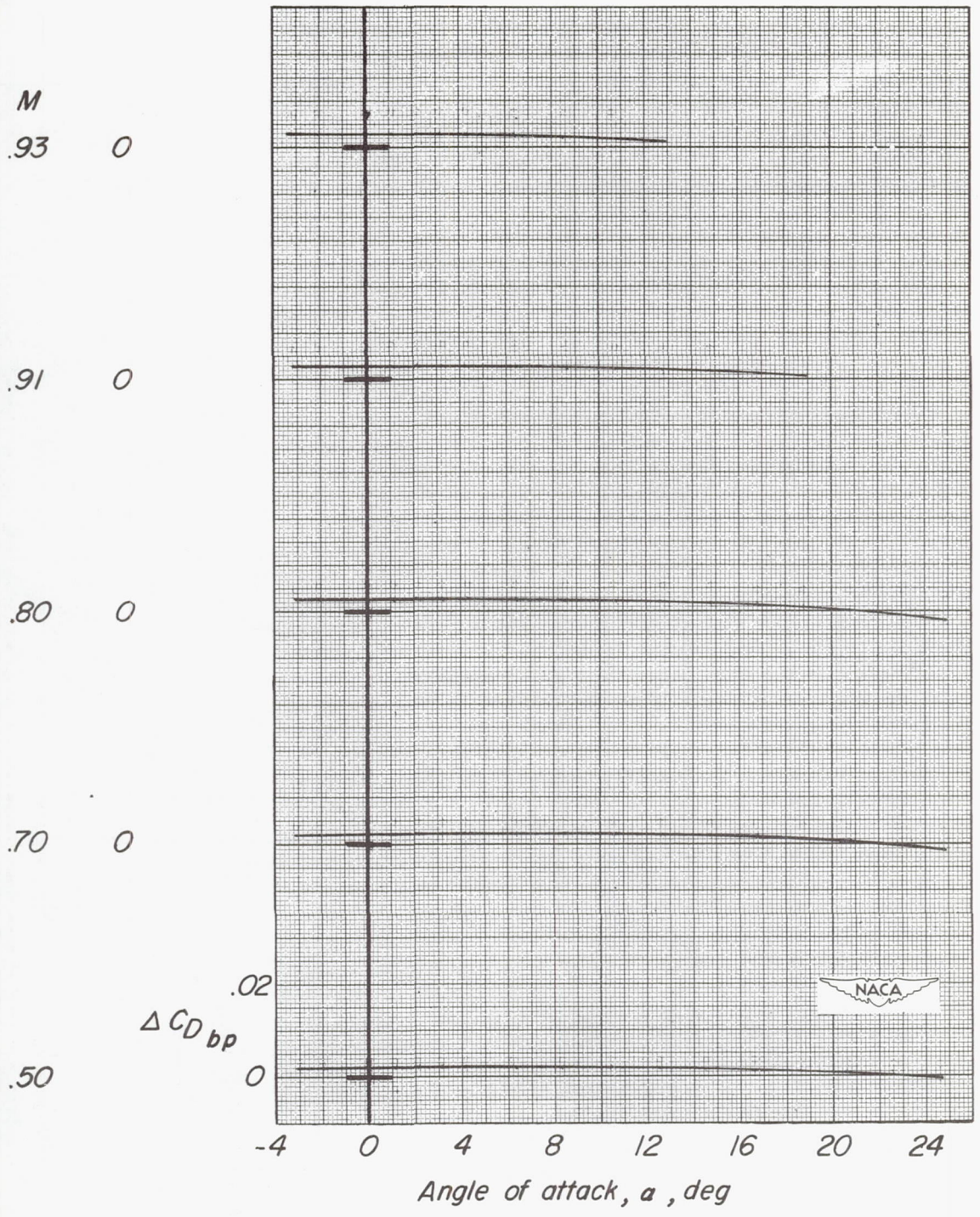

(b) $\Lambda = 45^\circ$.

Figure 6.- Concluded.

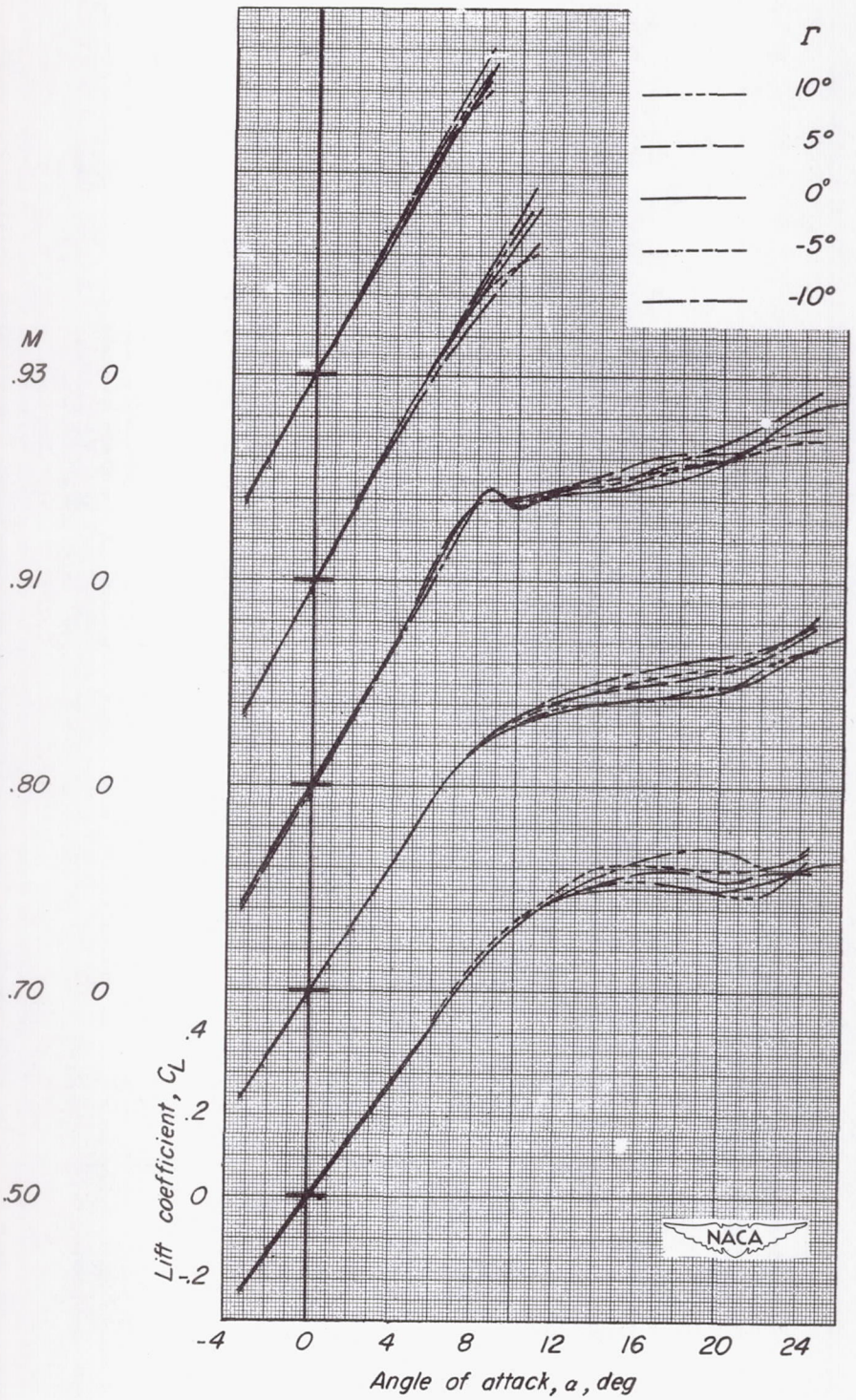

(a) $\Lambda = 3.6^{\circ}$.

Figure 7.- Effect of Mach number and dihedral angle on lift coefficient. $\beta = 0^{\circ}$.

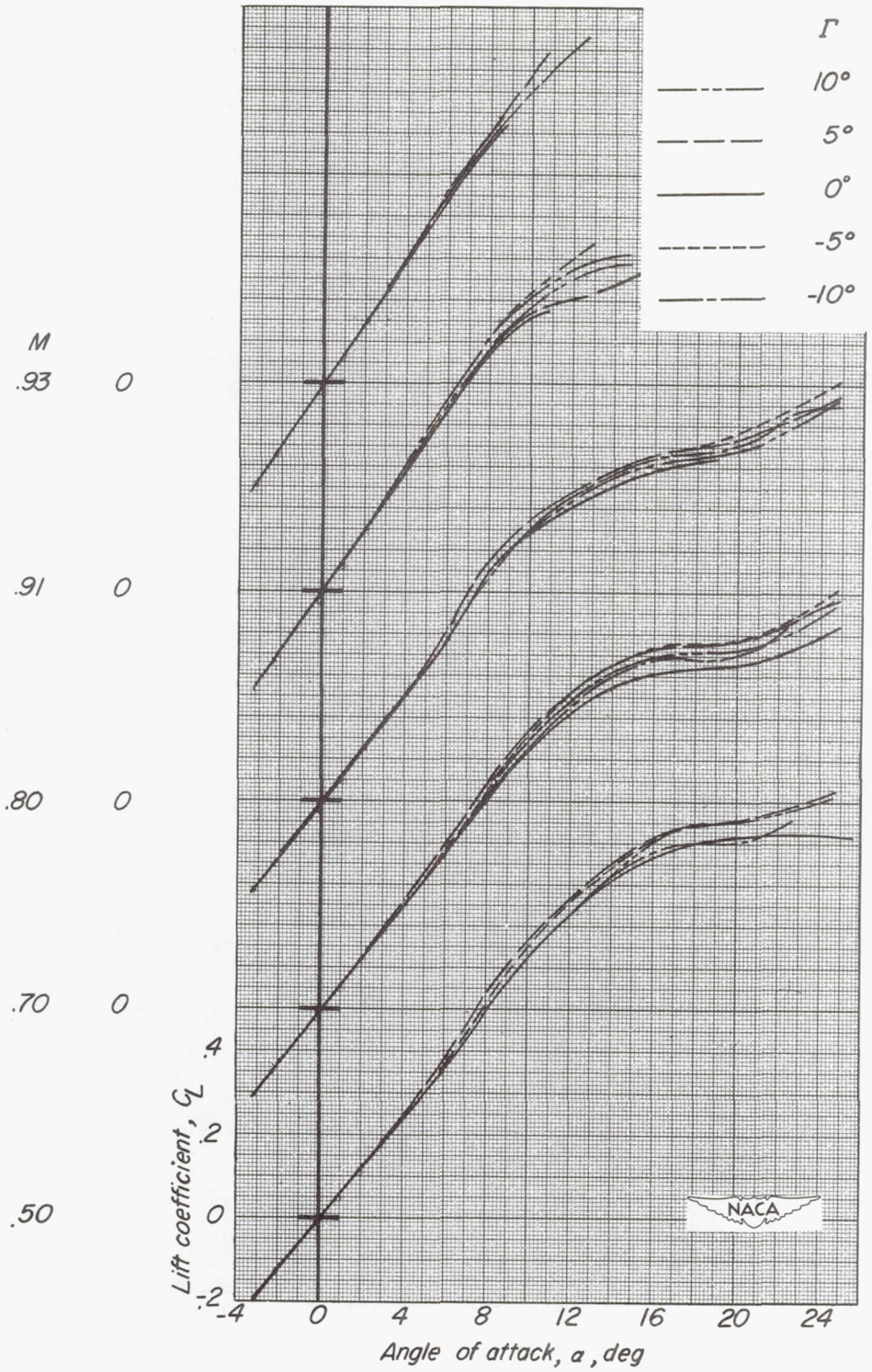

(b) $\Lambda = 45°$.

Figure 7.- Concluded.

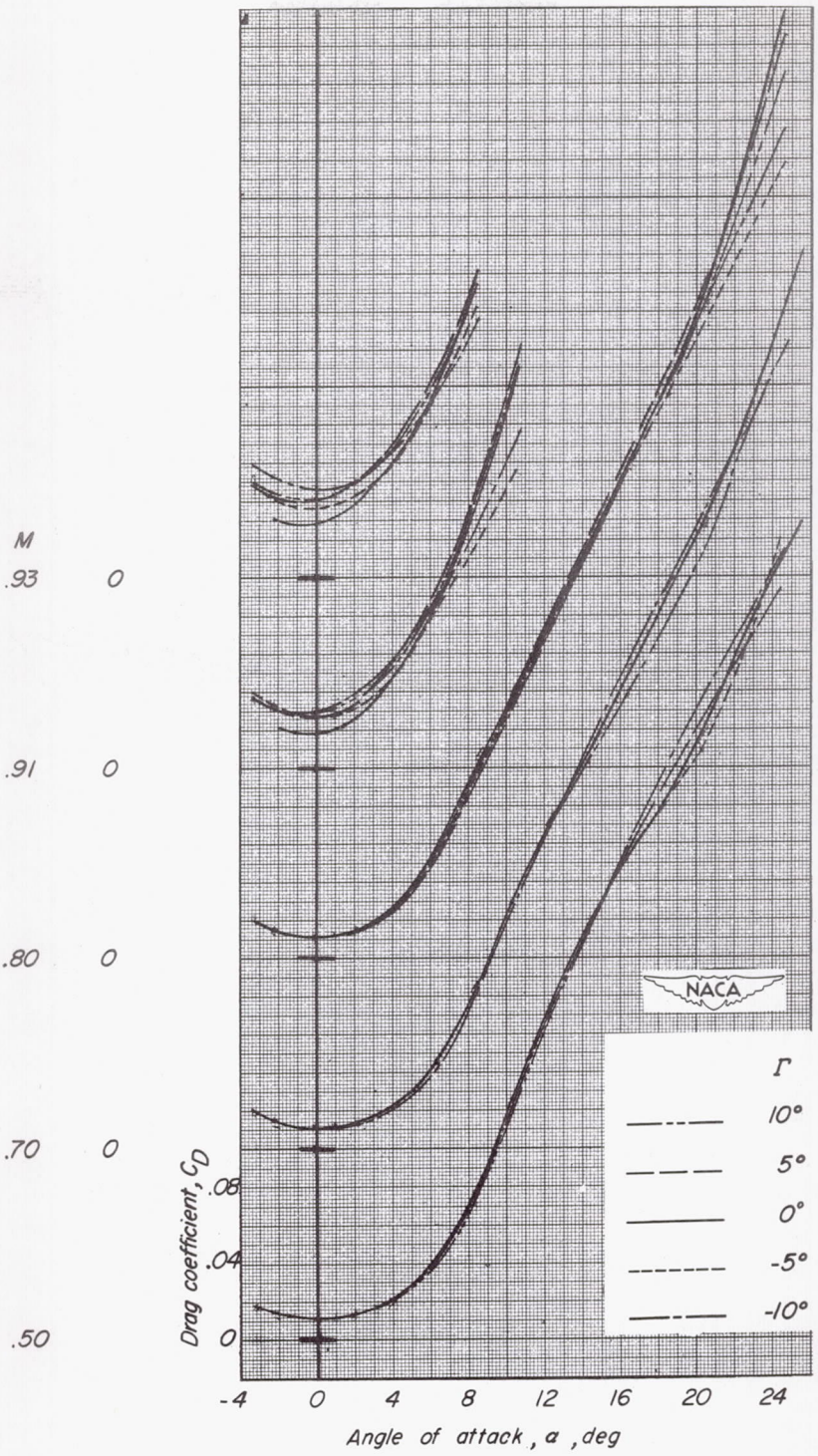

(a) $\Lambda = 3.6^{\circ}$.

Figure 8.- Effect of Mach number and dihedral angle on drag coefficient. $\beta = 0^{\circ}$.

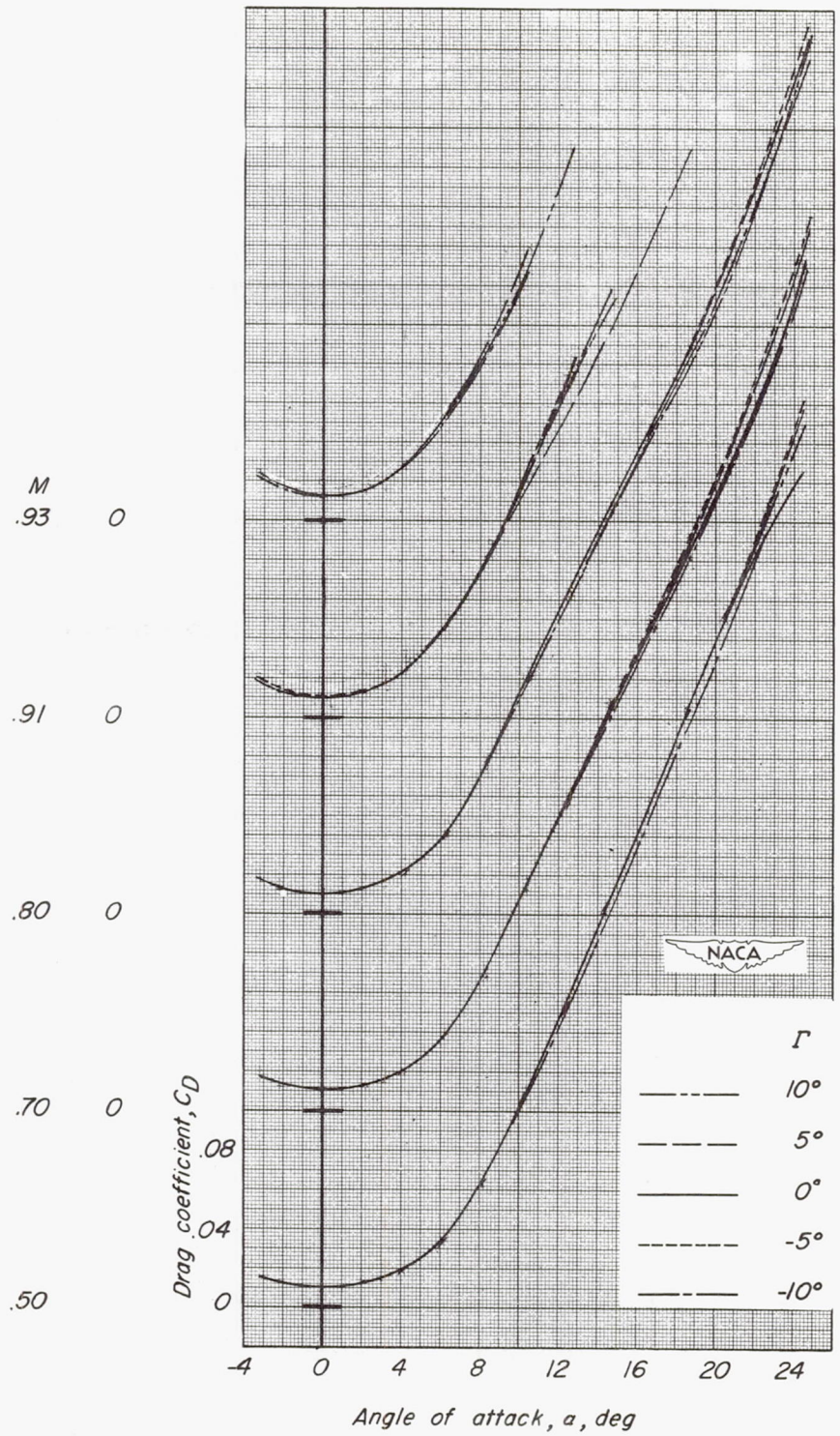

(b) $\Lambda = 45°$.

Figure 8.- Concluded.

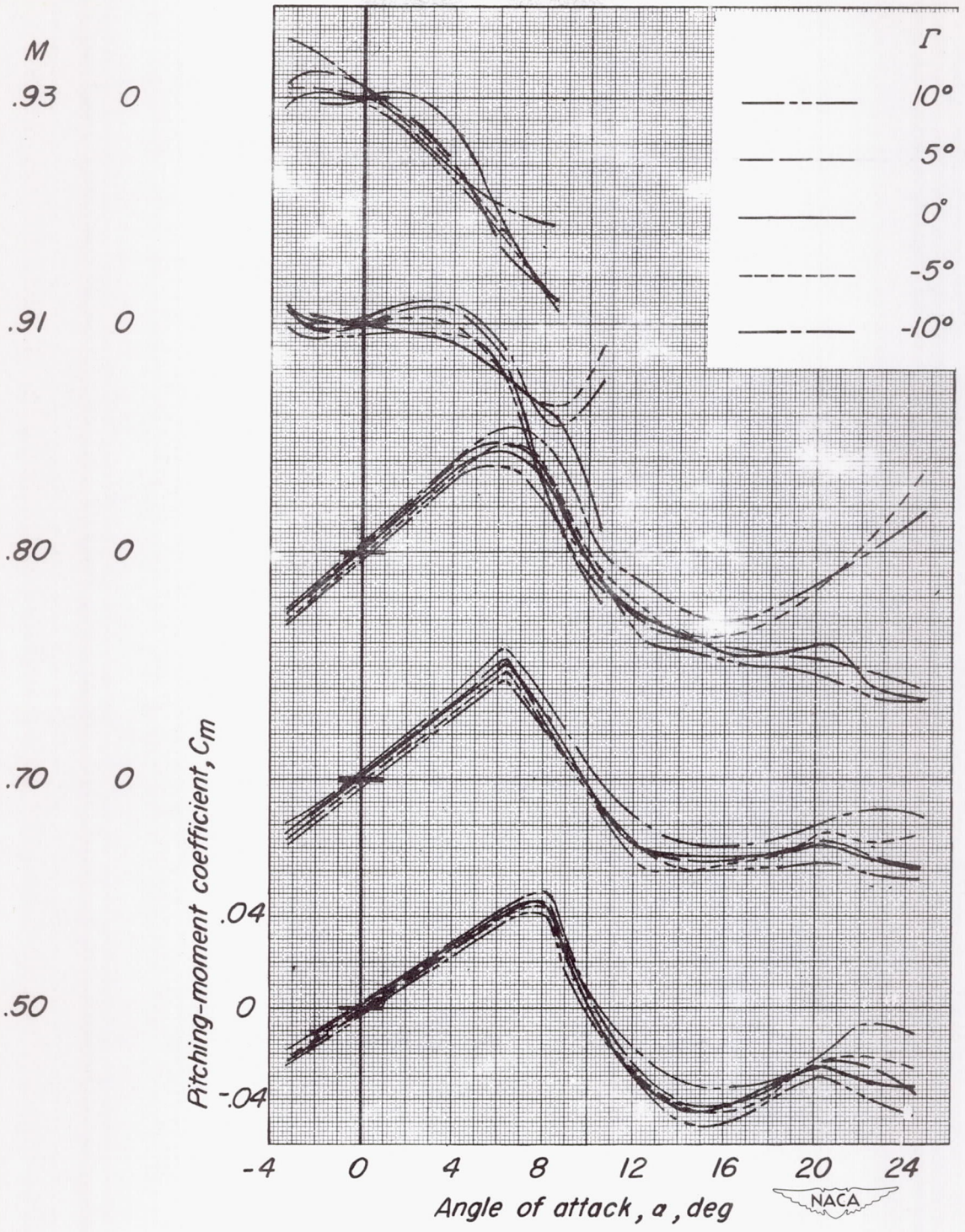

(a) $\Lambda = 3.6^{\circ}$.

Figure 9.- Effect of Mach number and dihedral angle on pitching-moment coefficient. $\beta = 0^{\circ}$.

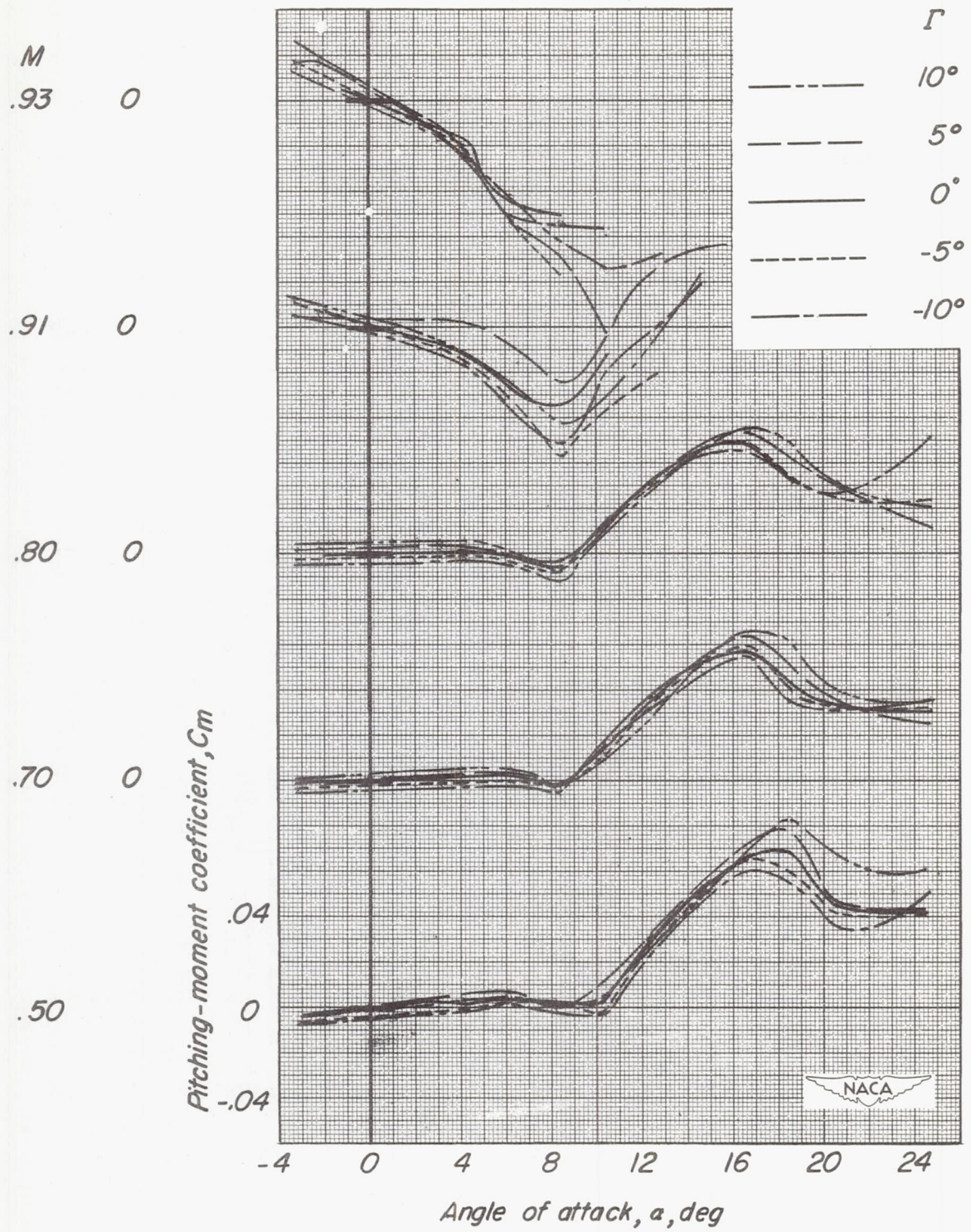

(b) $\Lambda = 45^{\circ}$.

Figure 9.- Concluded.

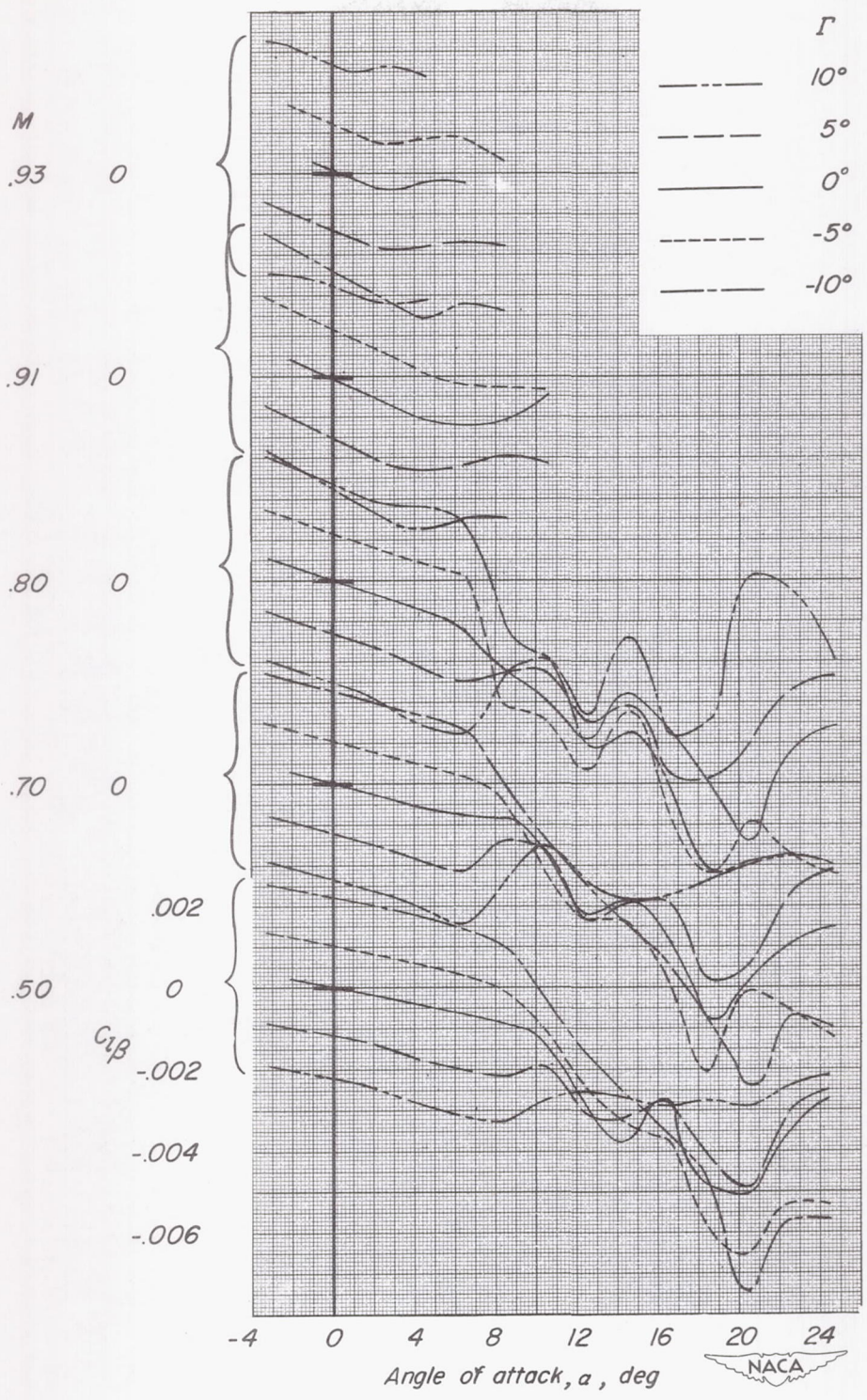

(a) $\Lambda = 3.6^\circ$.

Figure 10.- Effect of Mach number and dihedral angle on C_{l_β}. $\beta = \pm 4^\circ$.

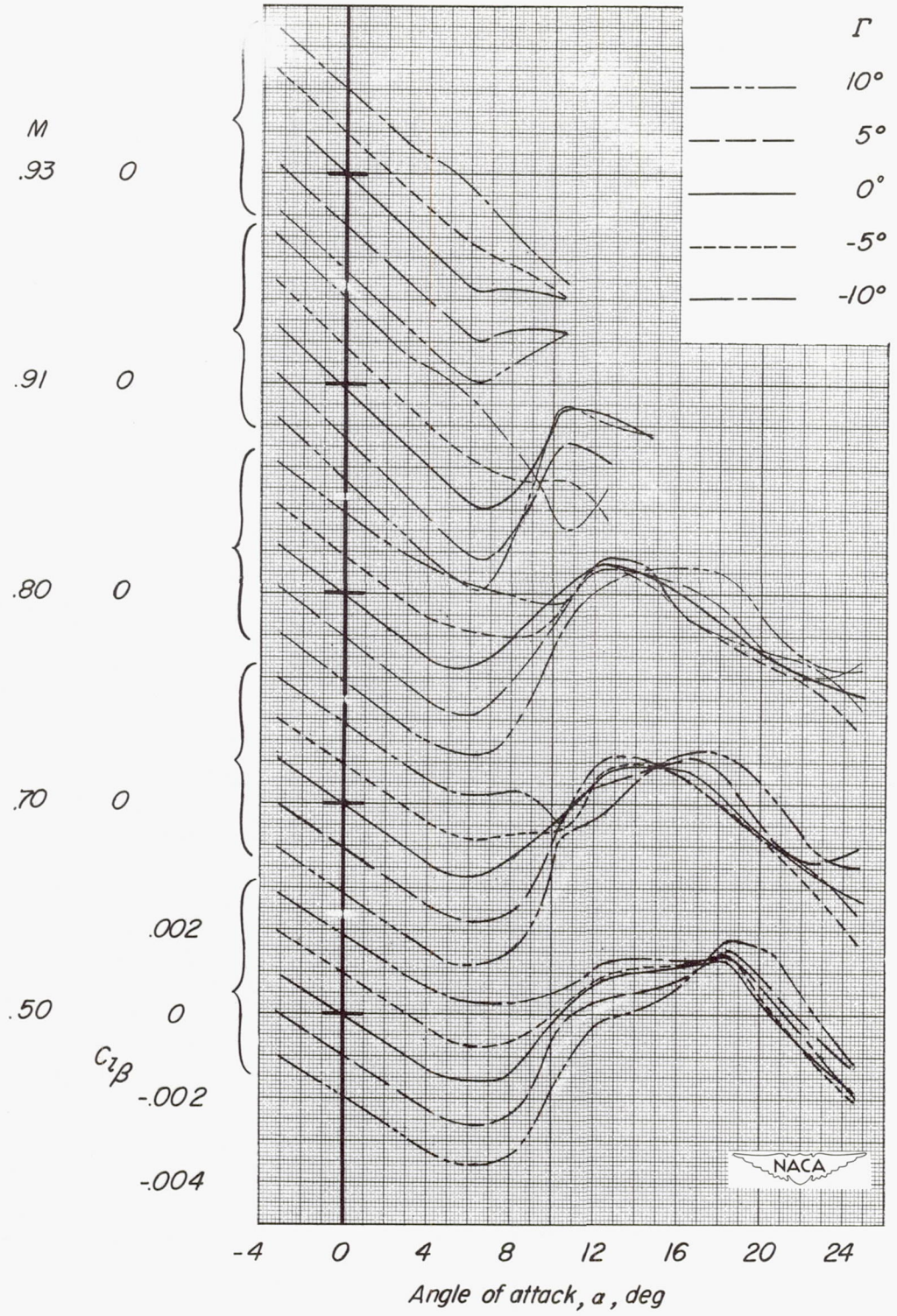

(b) $\Lambda = 45^\circ$.

Figure 10.- Concluded.

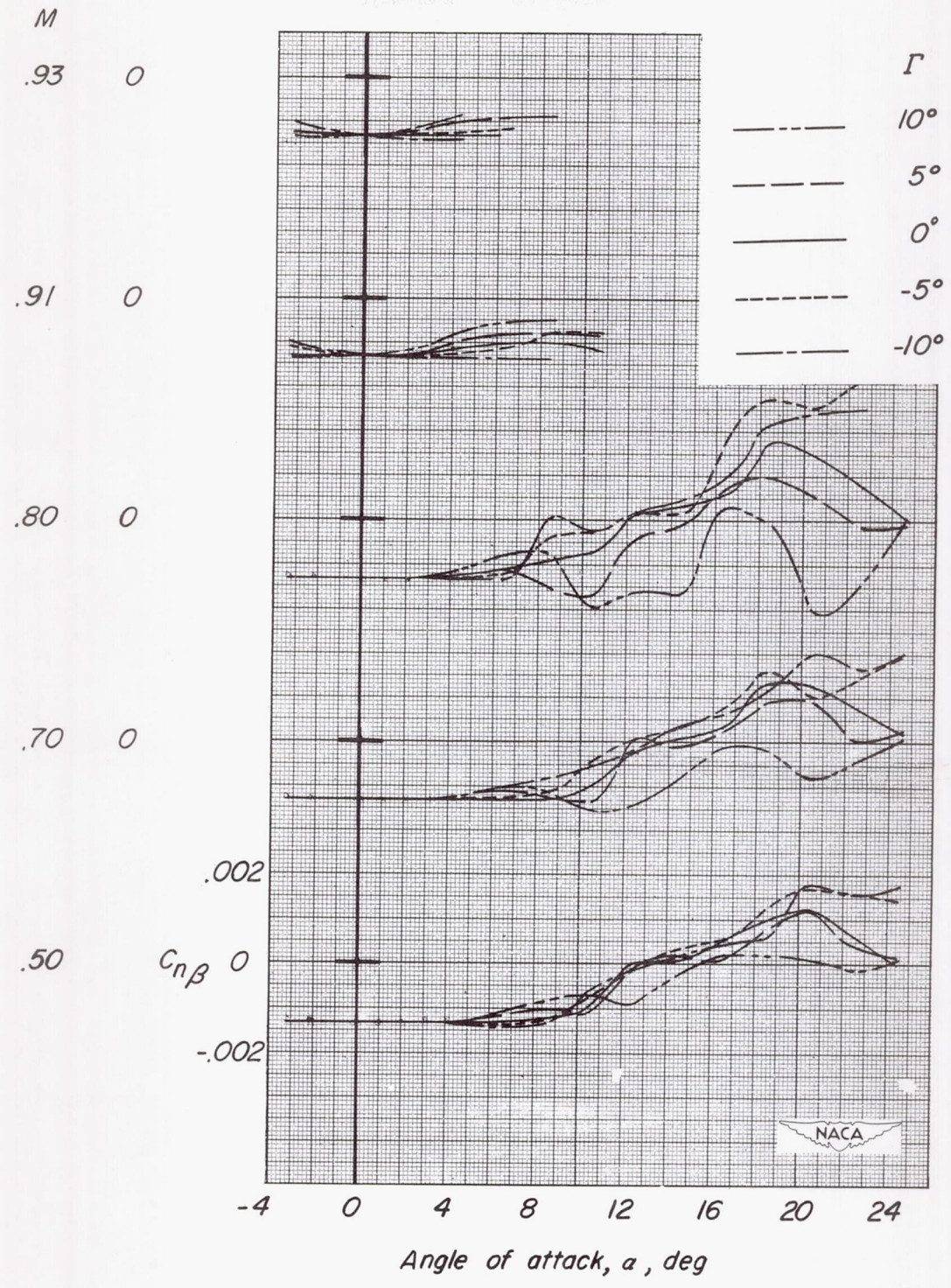

(a) $\Lambda = 3.6^\circ$.

Figure 11.- Effect of Mach number and dihedral angle on C_{n_β}. $\beta = \pm 4^\circ$.

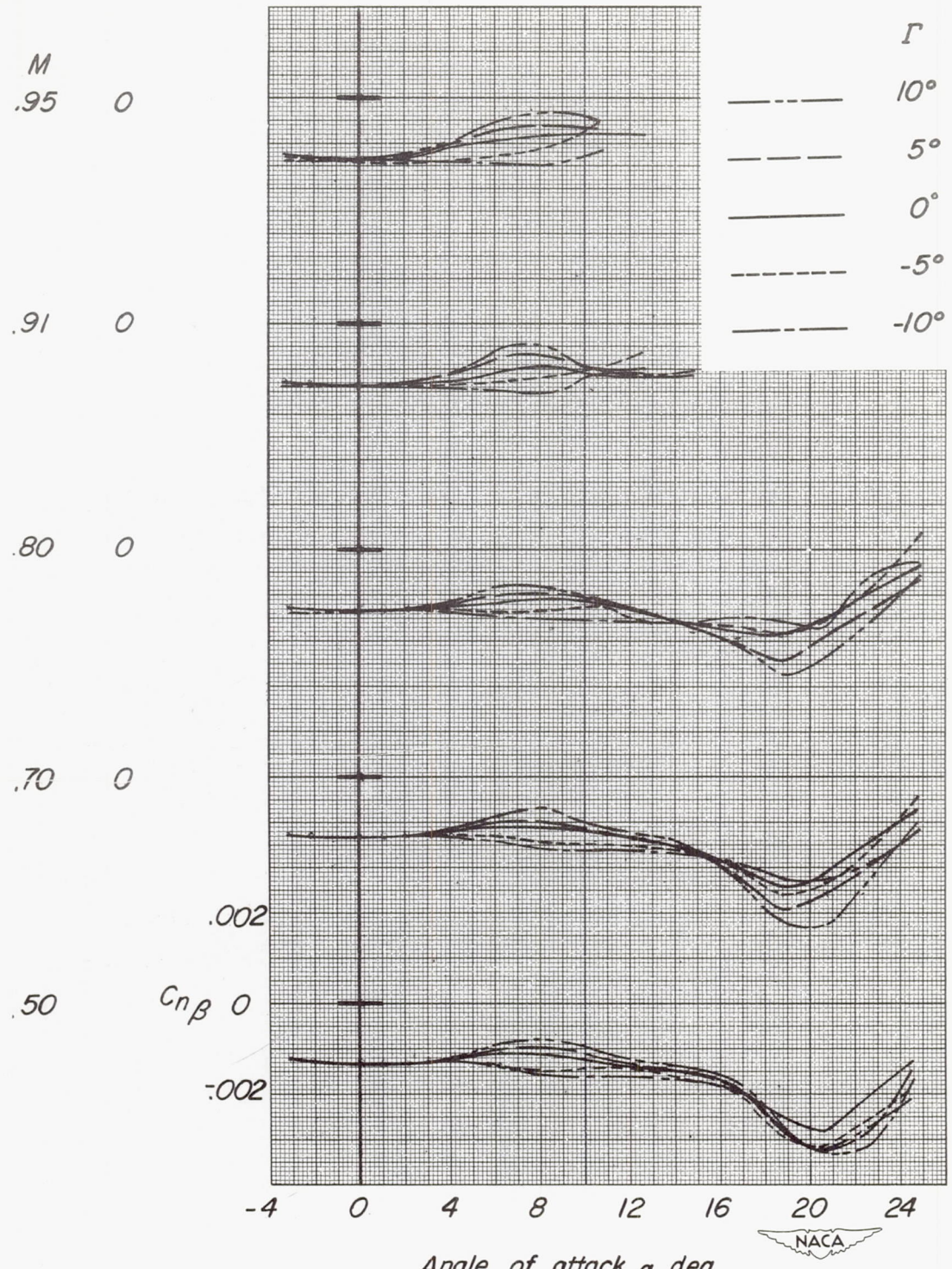

(b) $\Lambda = 45°$.

Figure 11.- Concluded.

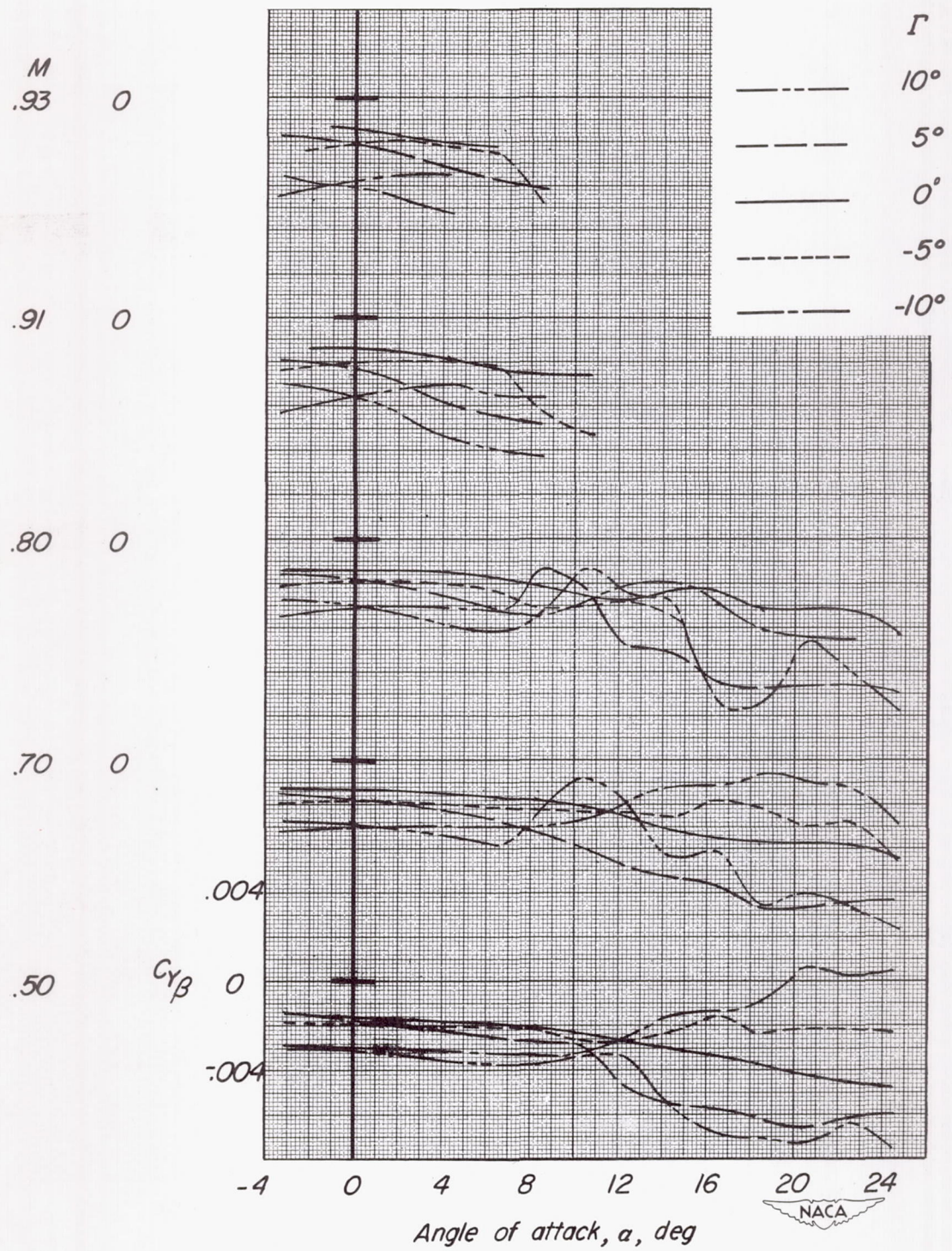

(a) $\Lambda = 3.6^\circ$.

Figure 12.- Effect of Mach number and dihedral angle on C_{Y_β}. $\beta = \pm 4^\circ$.

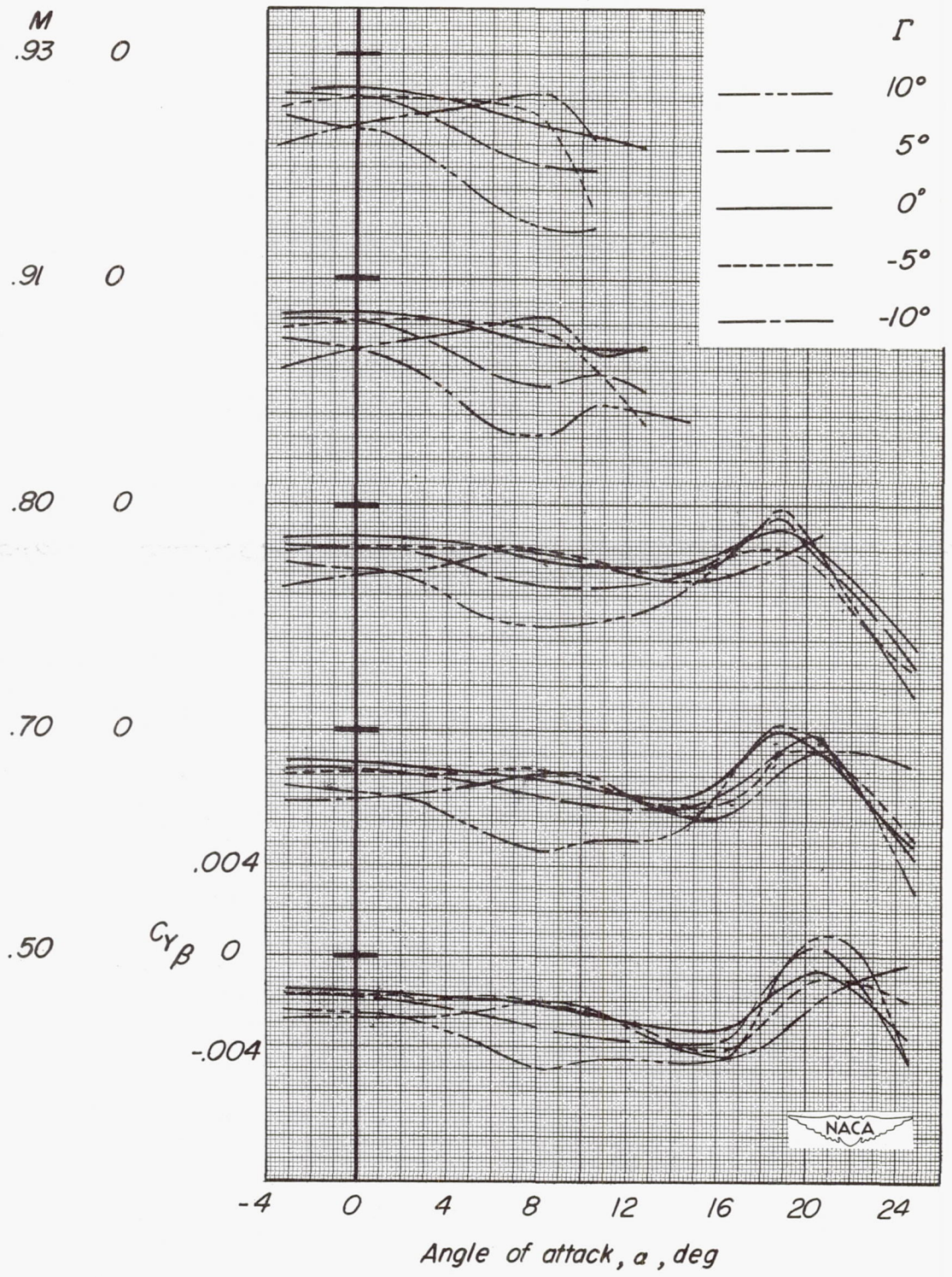

(b) $\Lambda = 45^\circ$.

Figure 12.- Concluded.

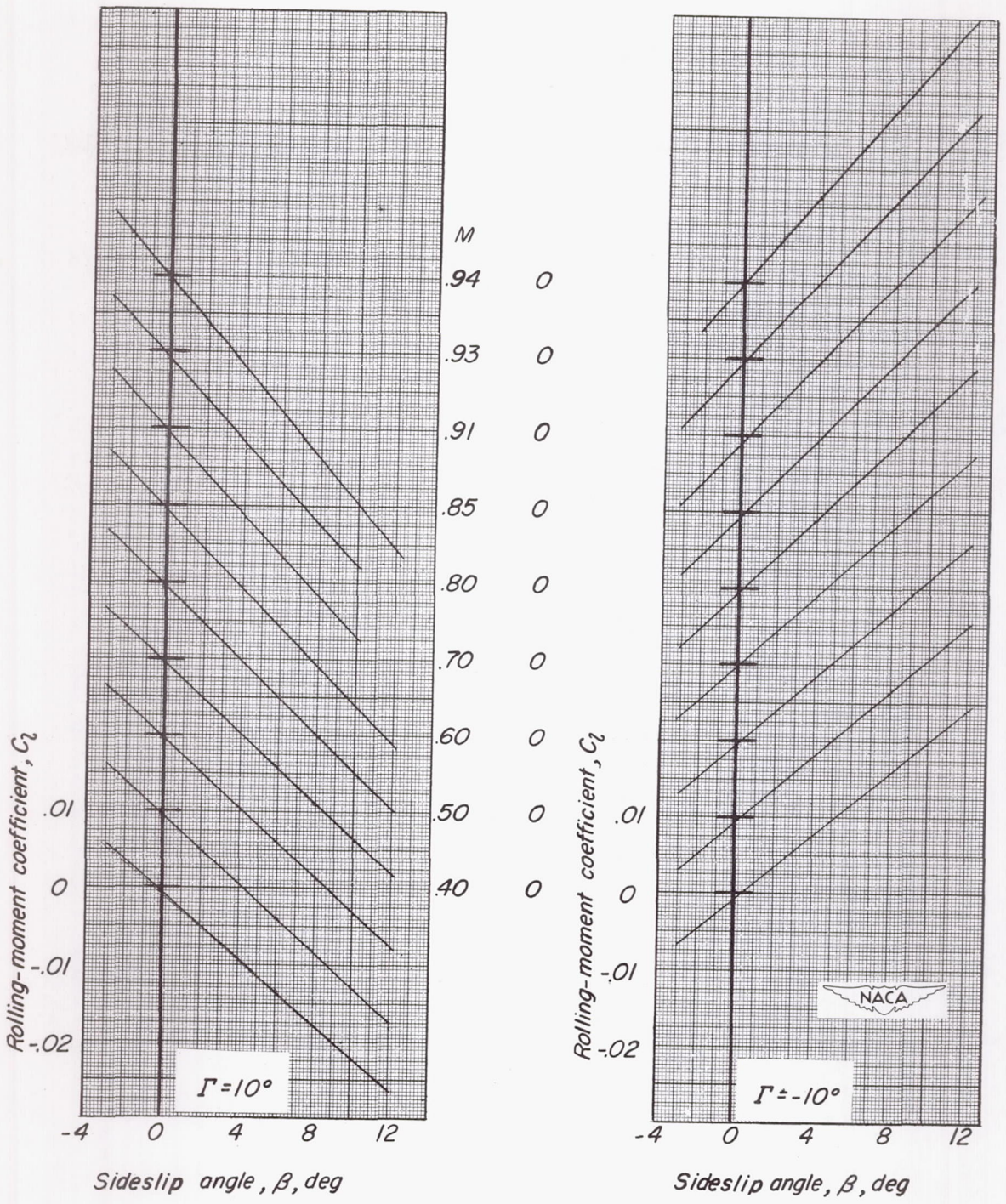

(a) $\Lambda = 3.6^{\circ}$.

Figure 13.- Effect of Mach number on the variation of rolling-moment coefficient C_l with sideslip angle β. $\alpha = 0^{\circ}$.

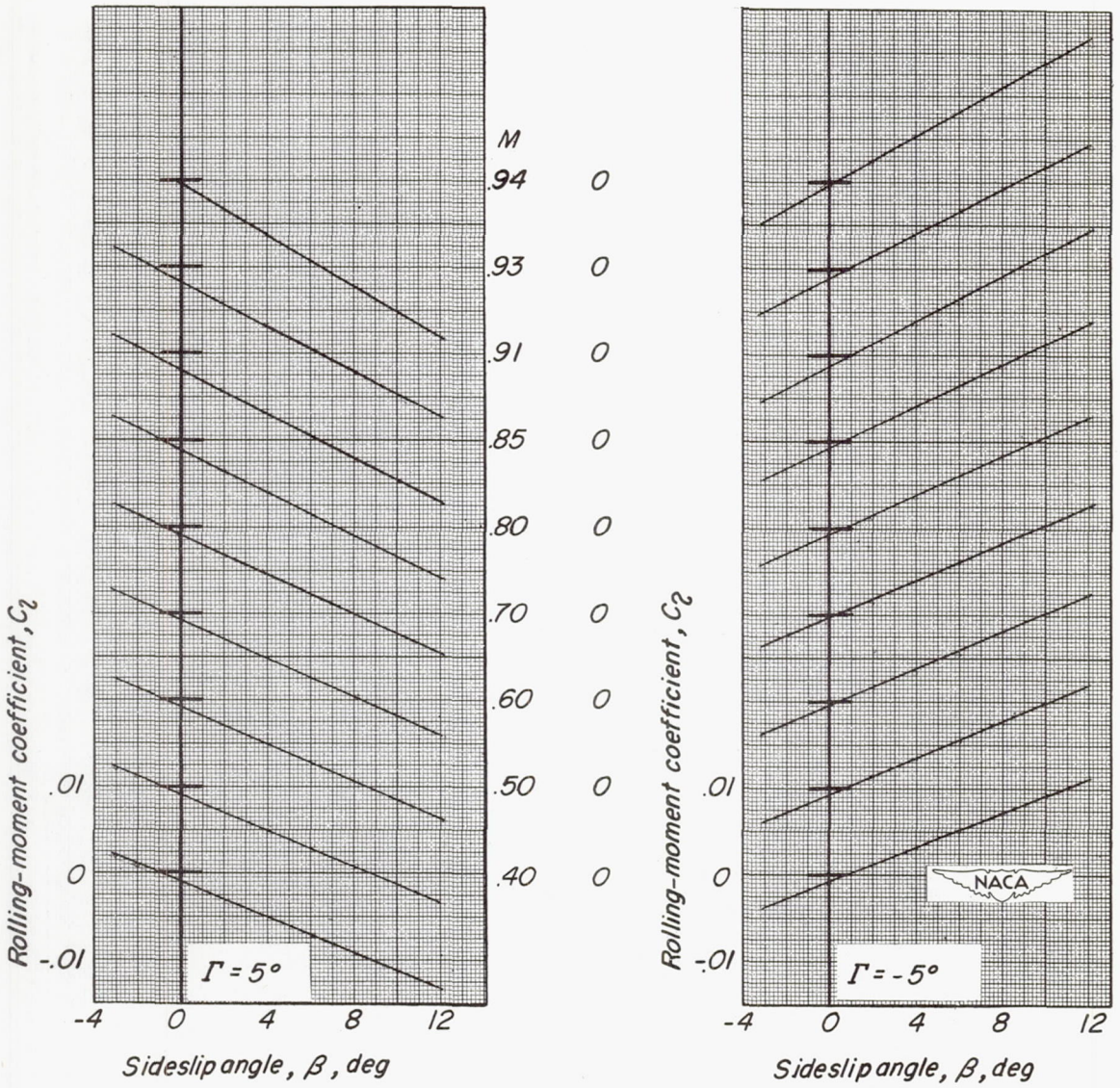

(a) Concluded.

Figure 13.- Continued.

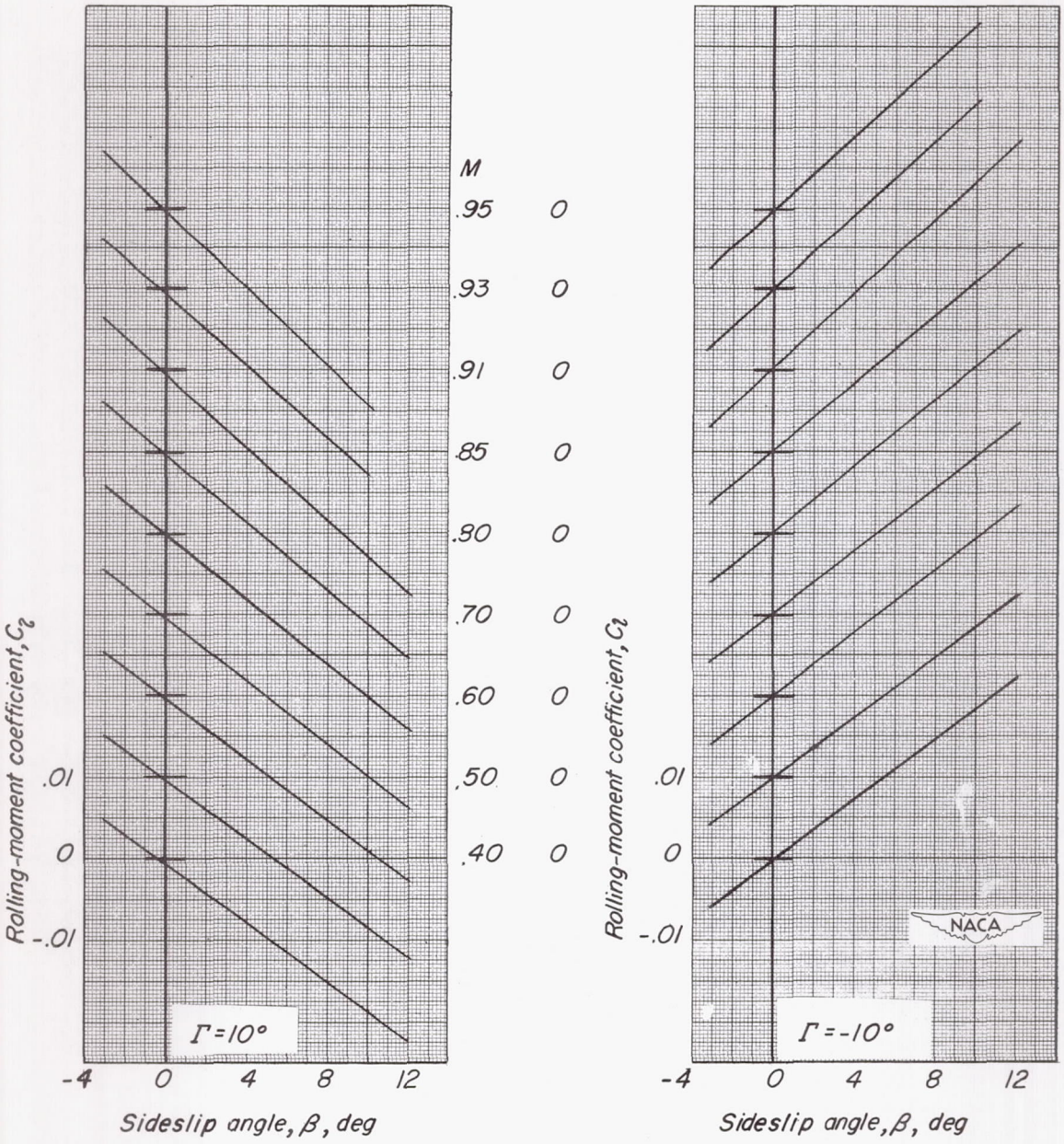

(b) $\Lambda = 45°$.

Figure 13.- Continued.

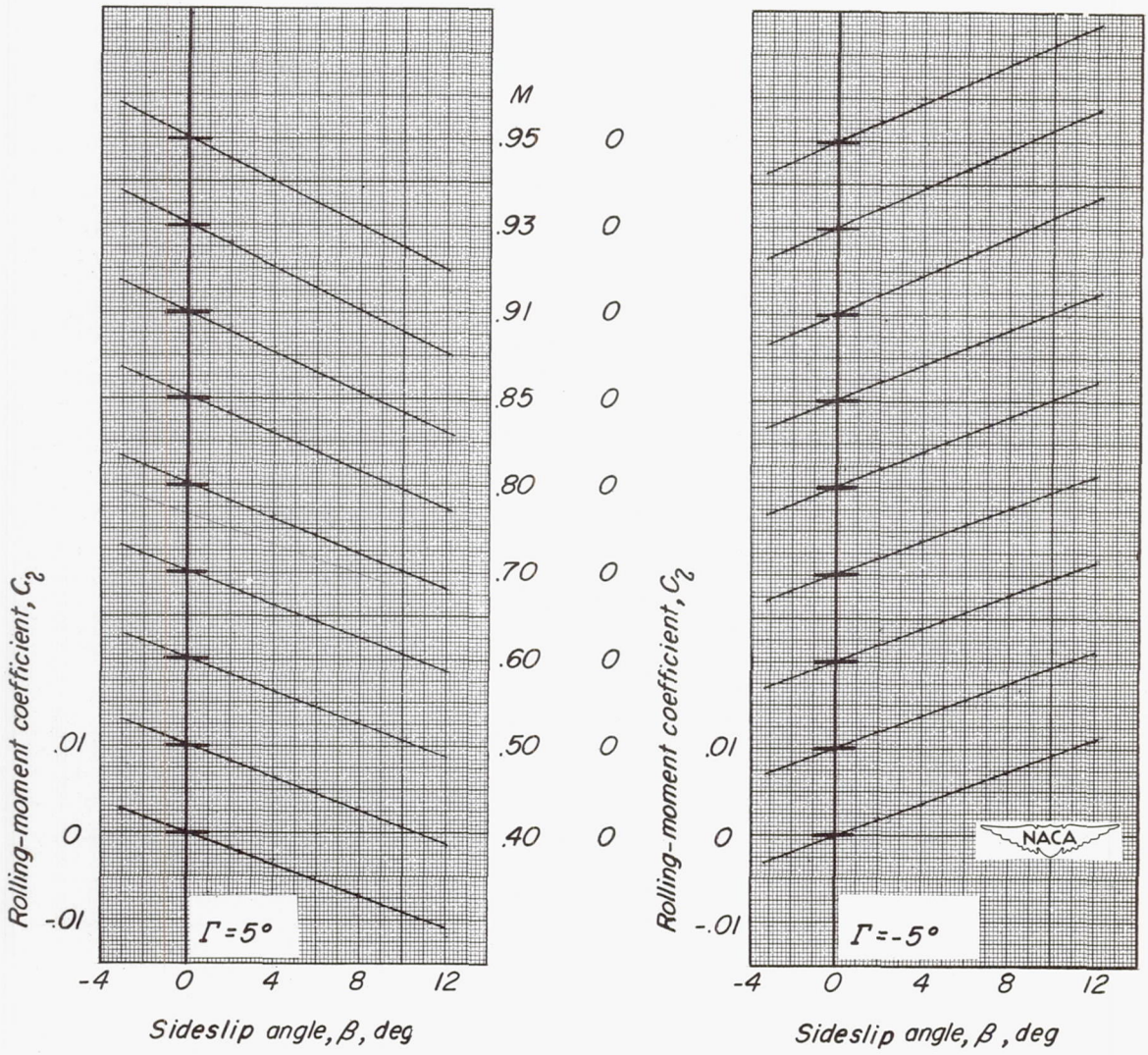

(b) Concluded.

Figure 13.- Concluded.

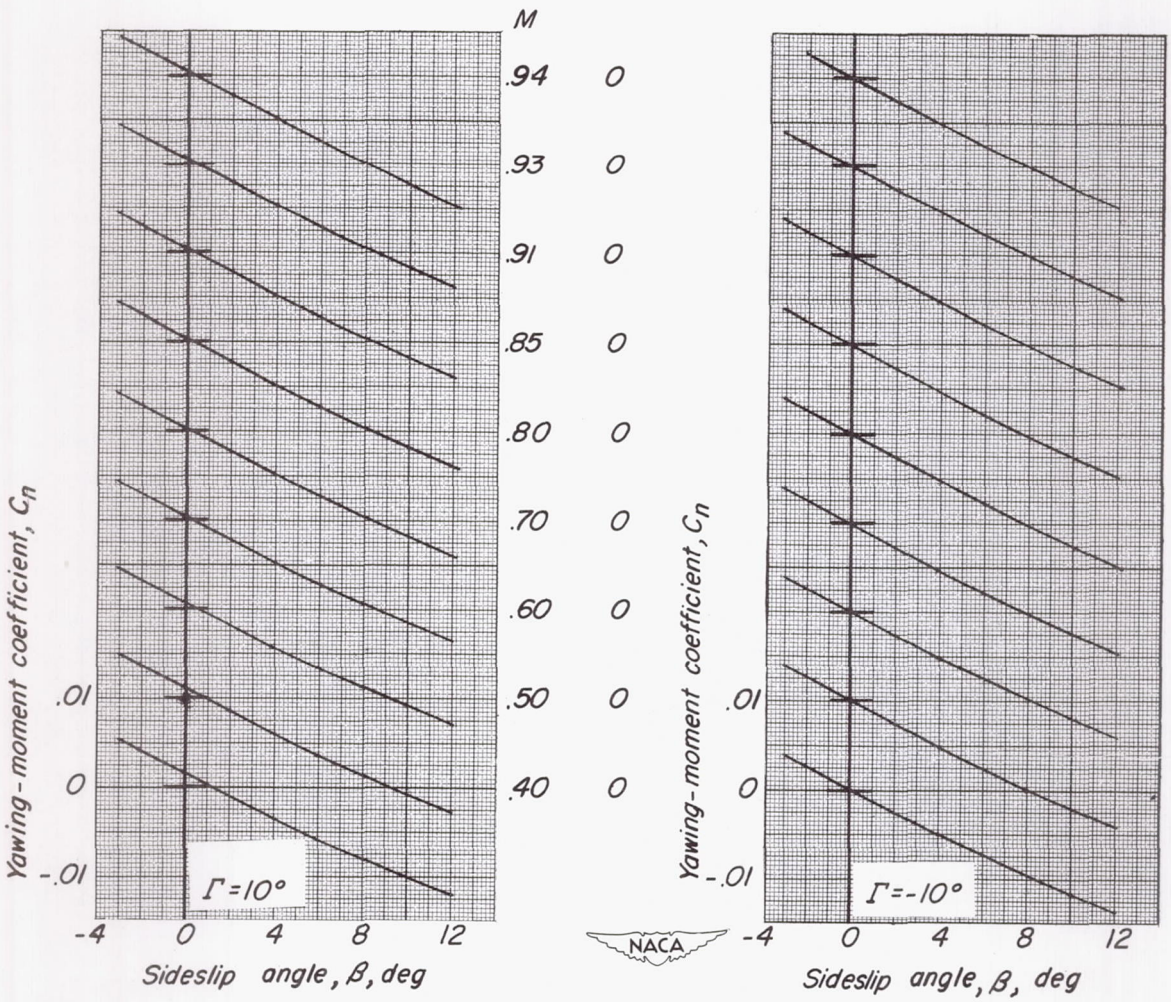

(a) $\Lambda = 3.6^{\circ}$.

Figure 14.- Effect of Mach number on the variation of yawing-moment coefficient C_n with sideslip angle β. $\alpha = 0^{\circ}$.

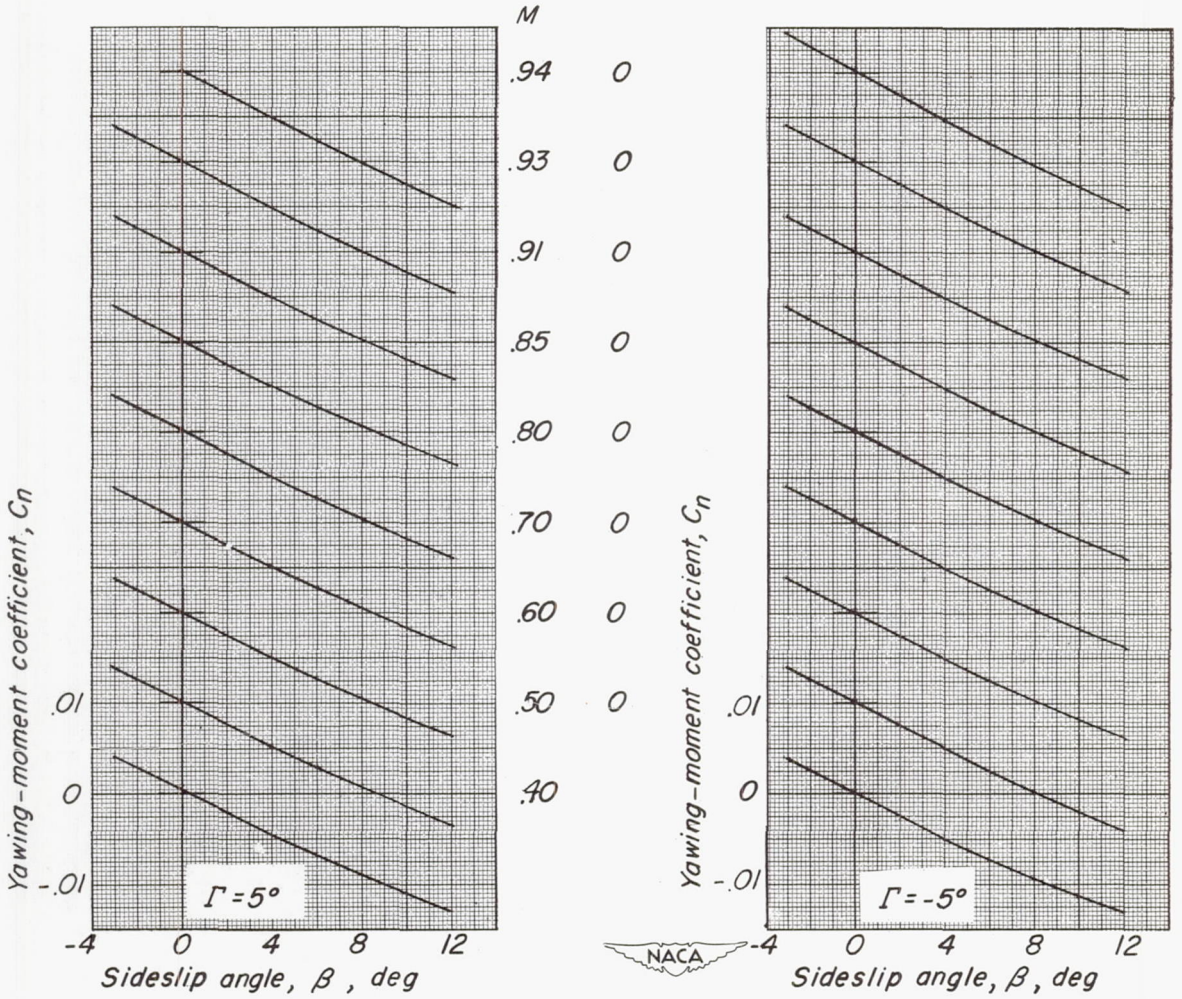

(a) Concluded.

Figure 14.- Continued.

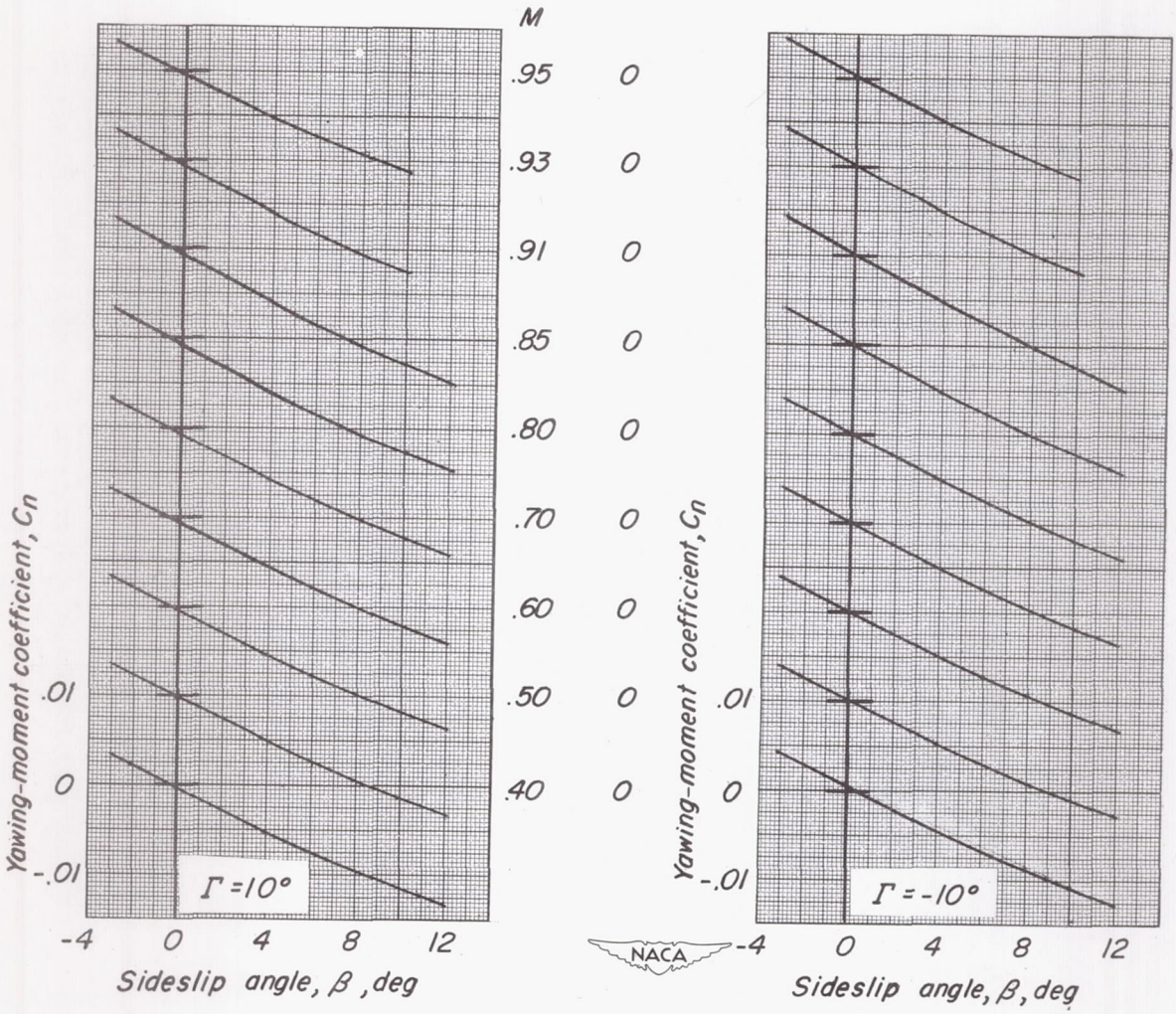

(b) $\Lambda = 45°$.

Figure 14.- Continued.

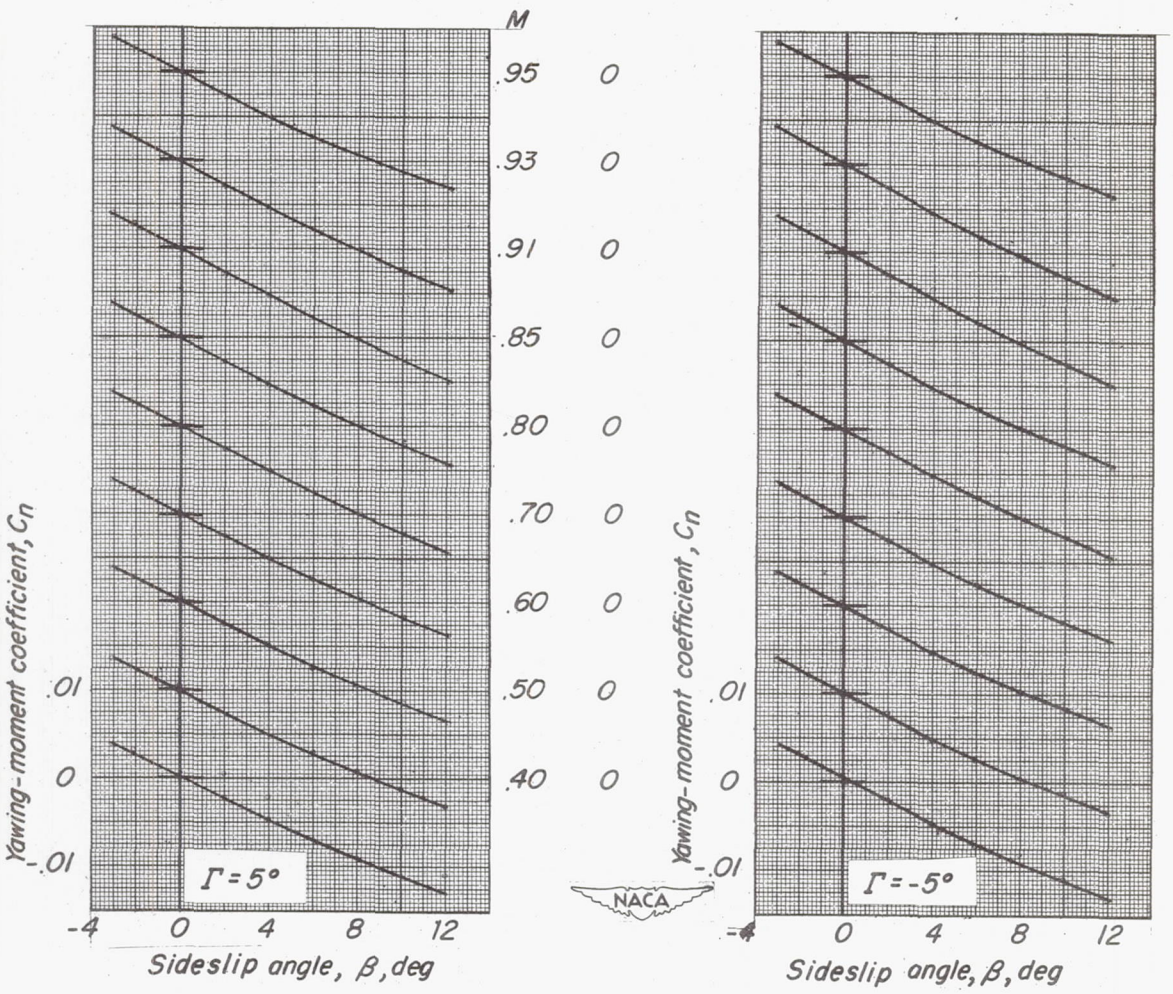

(b) Concluded.

Figure 14.- Concluded.

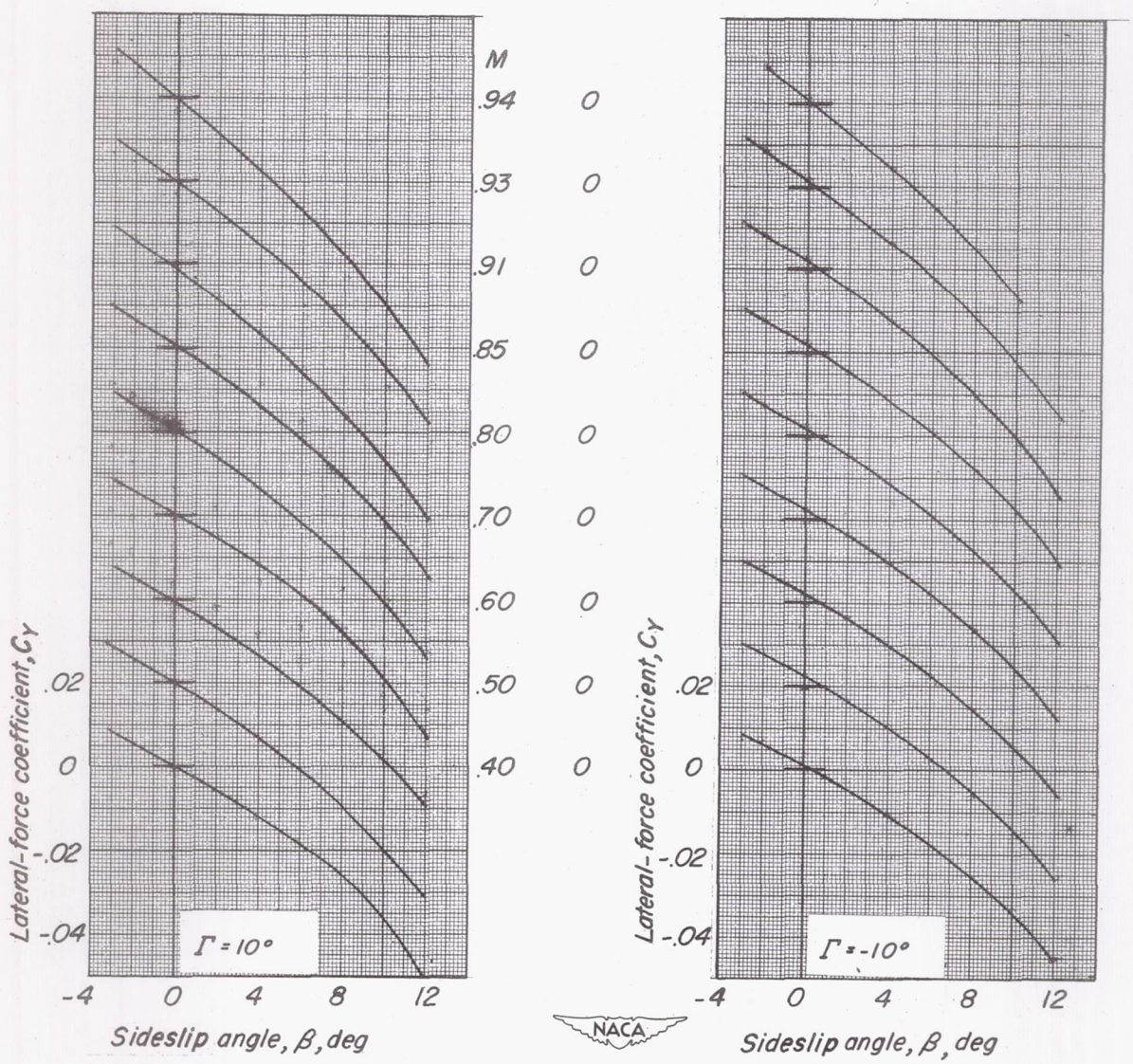

(a) $\Lambda = 3.6°$.

Figure 15.- Effect of Mach number on the variation of lateral-force coefficient C_Y with sideslip angle β. $\alpha = 0°$.

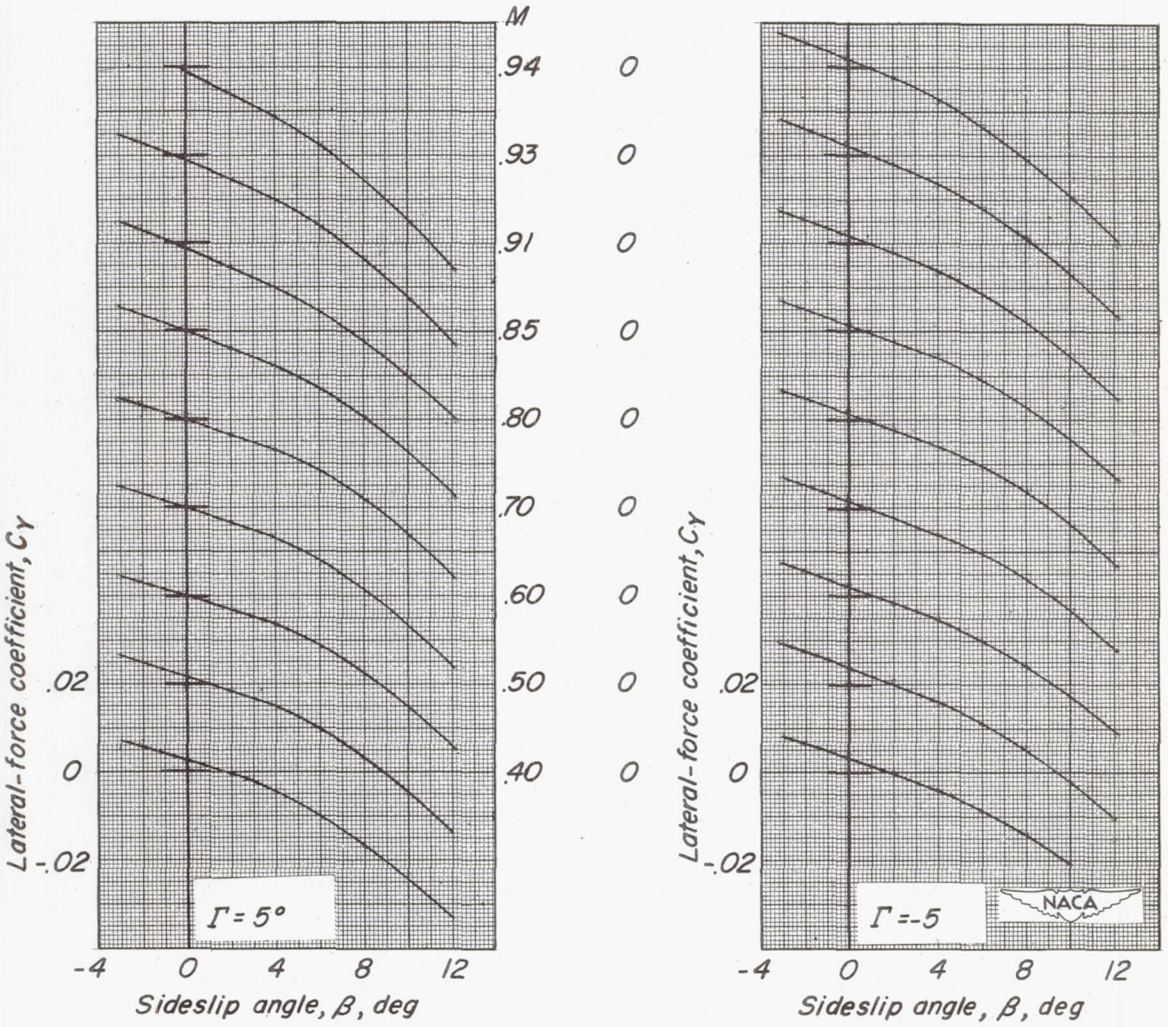

(a) Concluded.

Figure 15.- Continued.

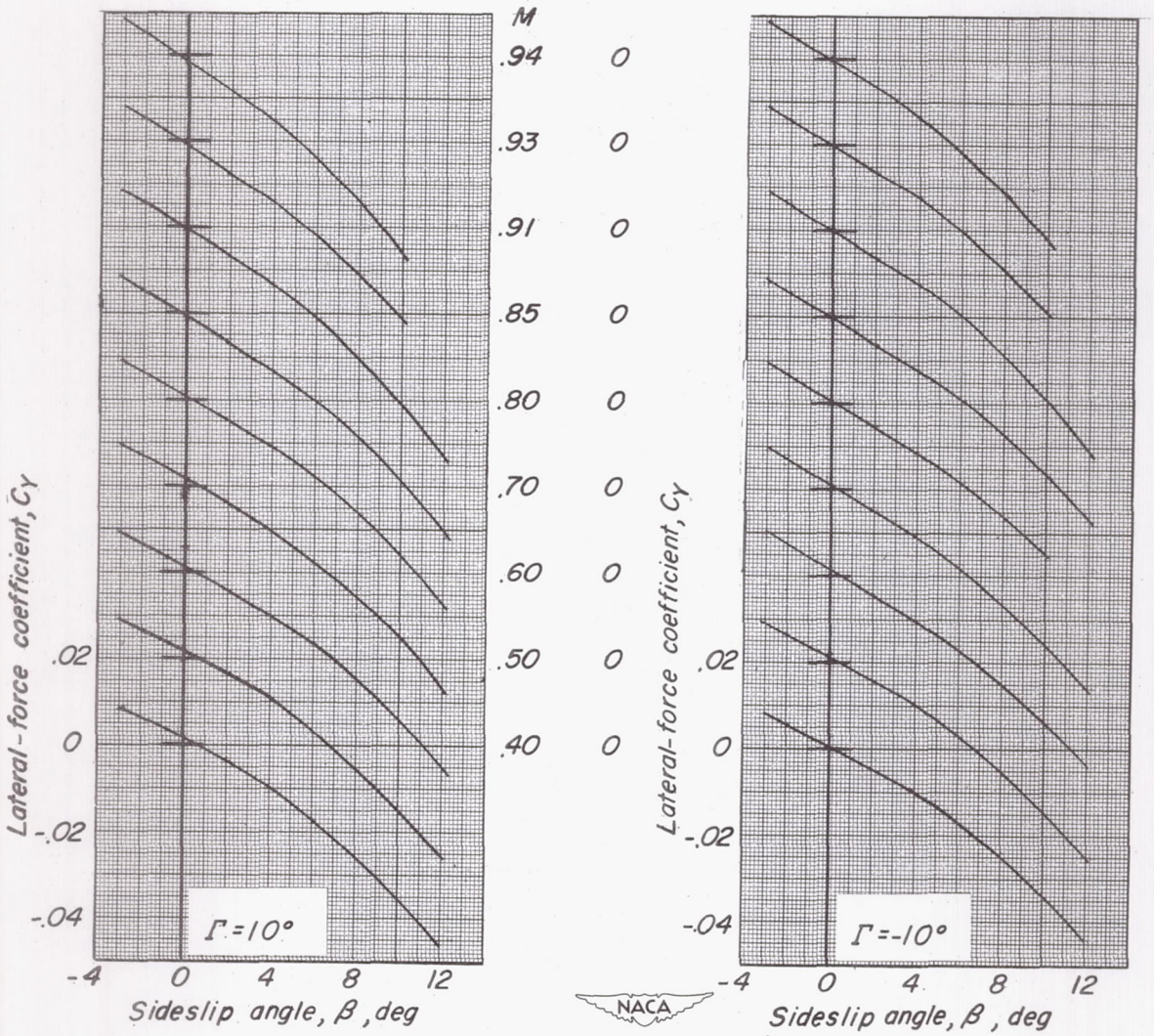

(b) $\Lambda = 45°$.

Figure 15.- Continued.

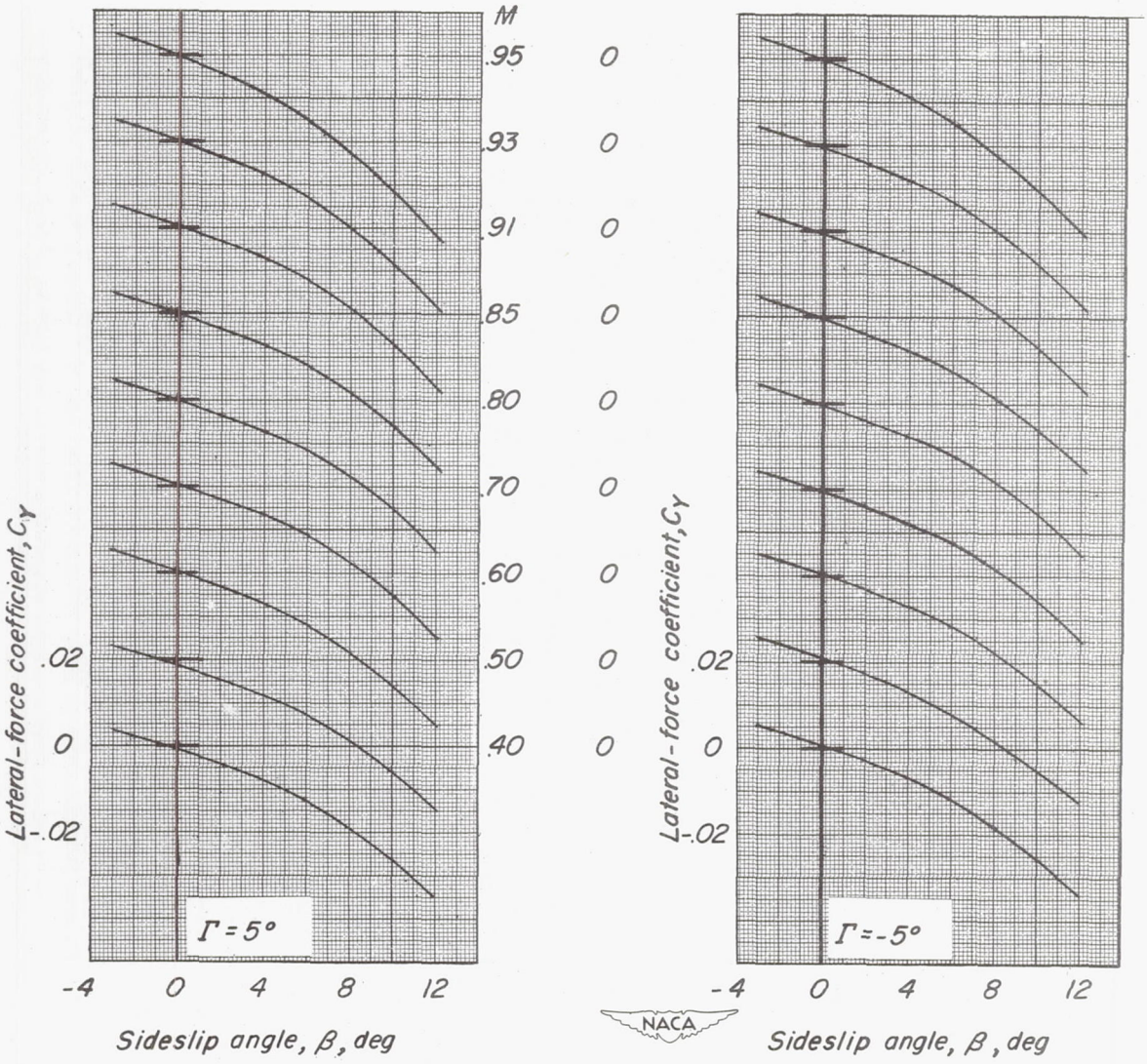

(b) Concluded.

Figure 15.- Concluded.

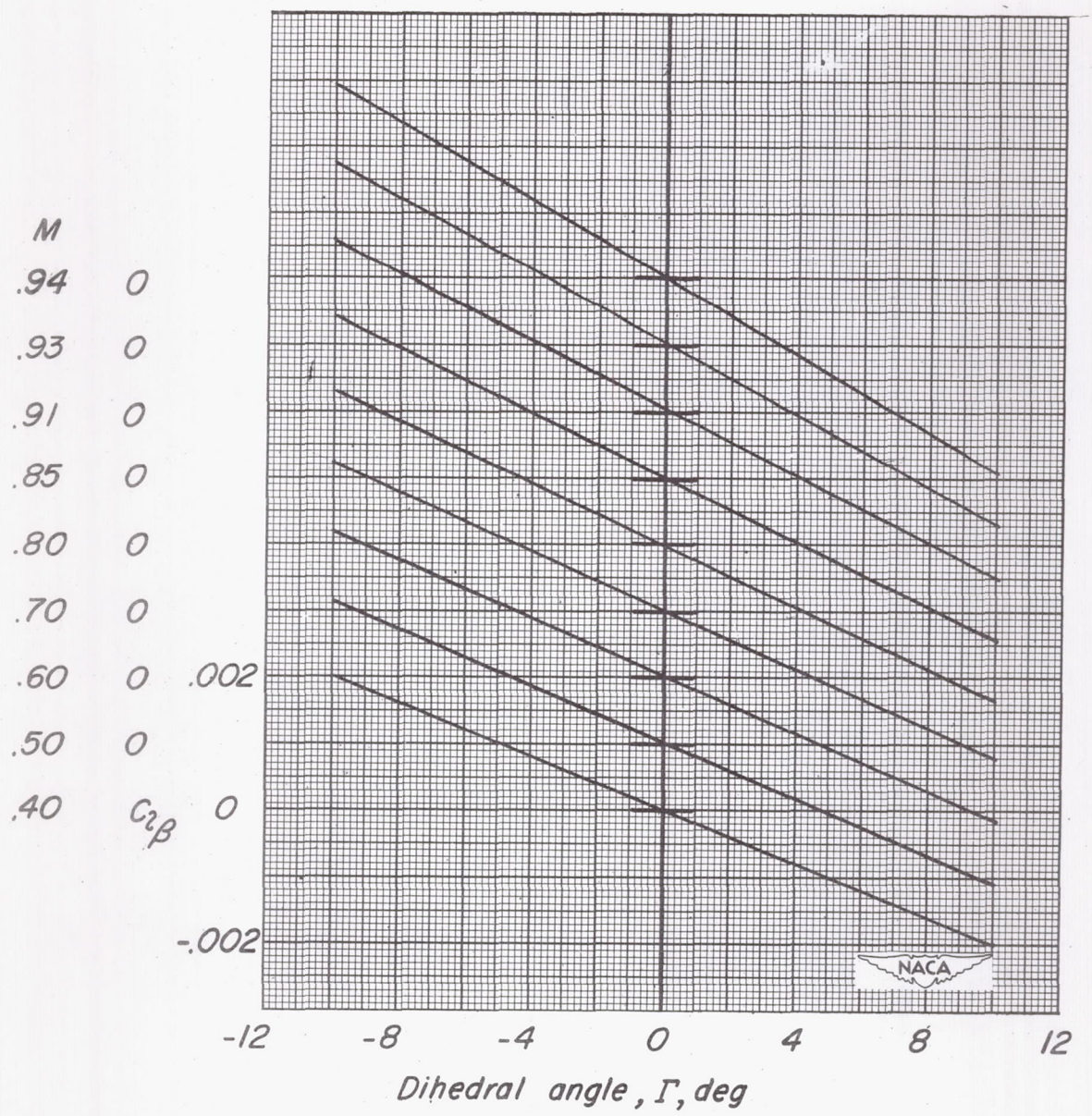

(a) $\Lambda = 3.6^\circ$.

Figure 16.- Effect of Mach number on variation of C_{l_β} with dihedral angle Γ. $\alpha = 0^\circ$.

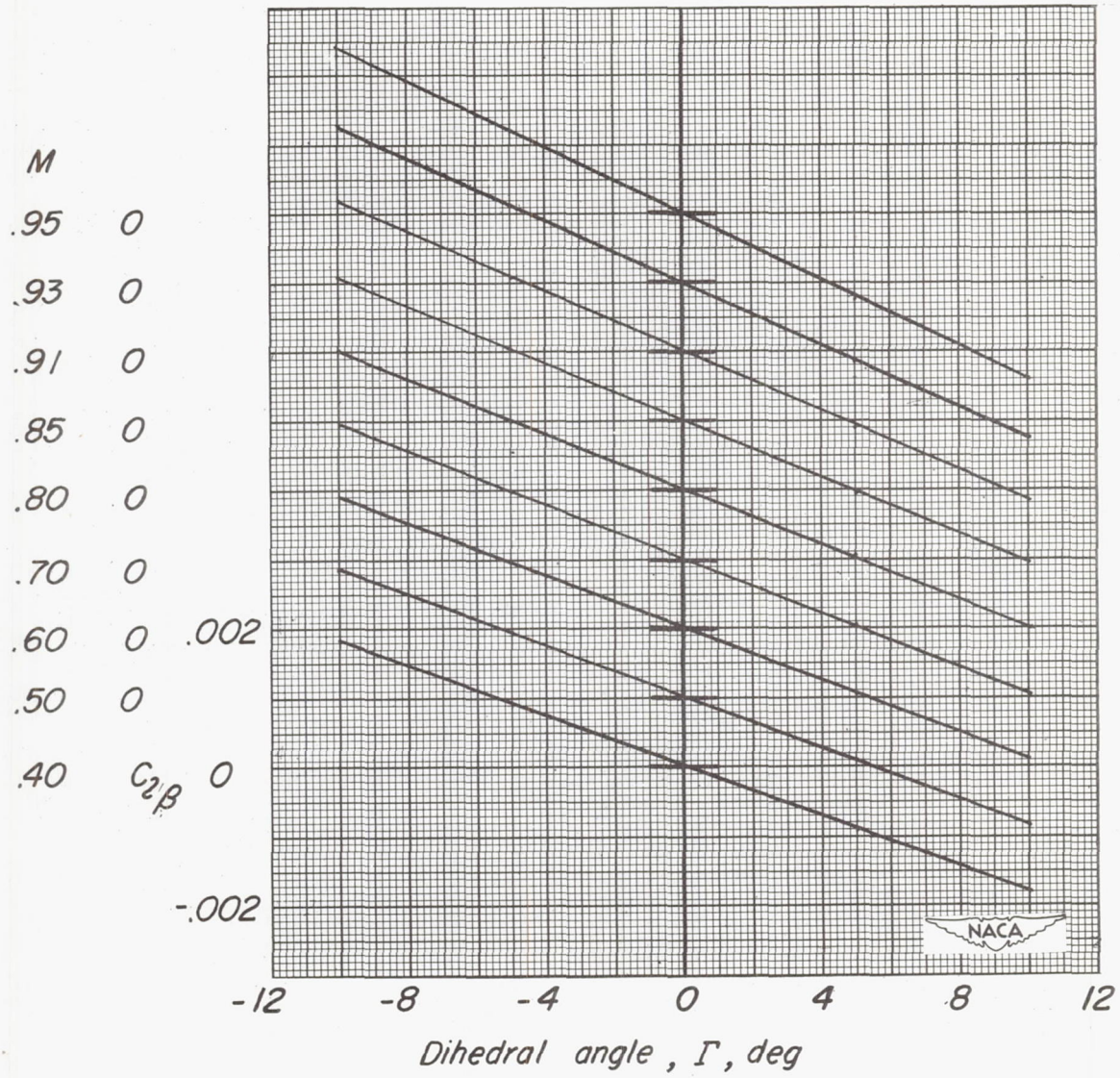

(b) $\Lambda = 45^\circ$.

Figure 16.- Concluded.

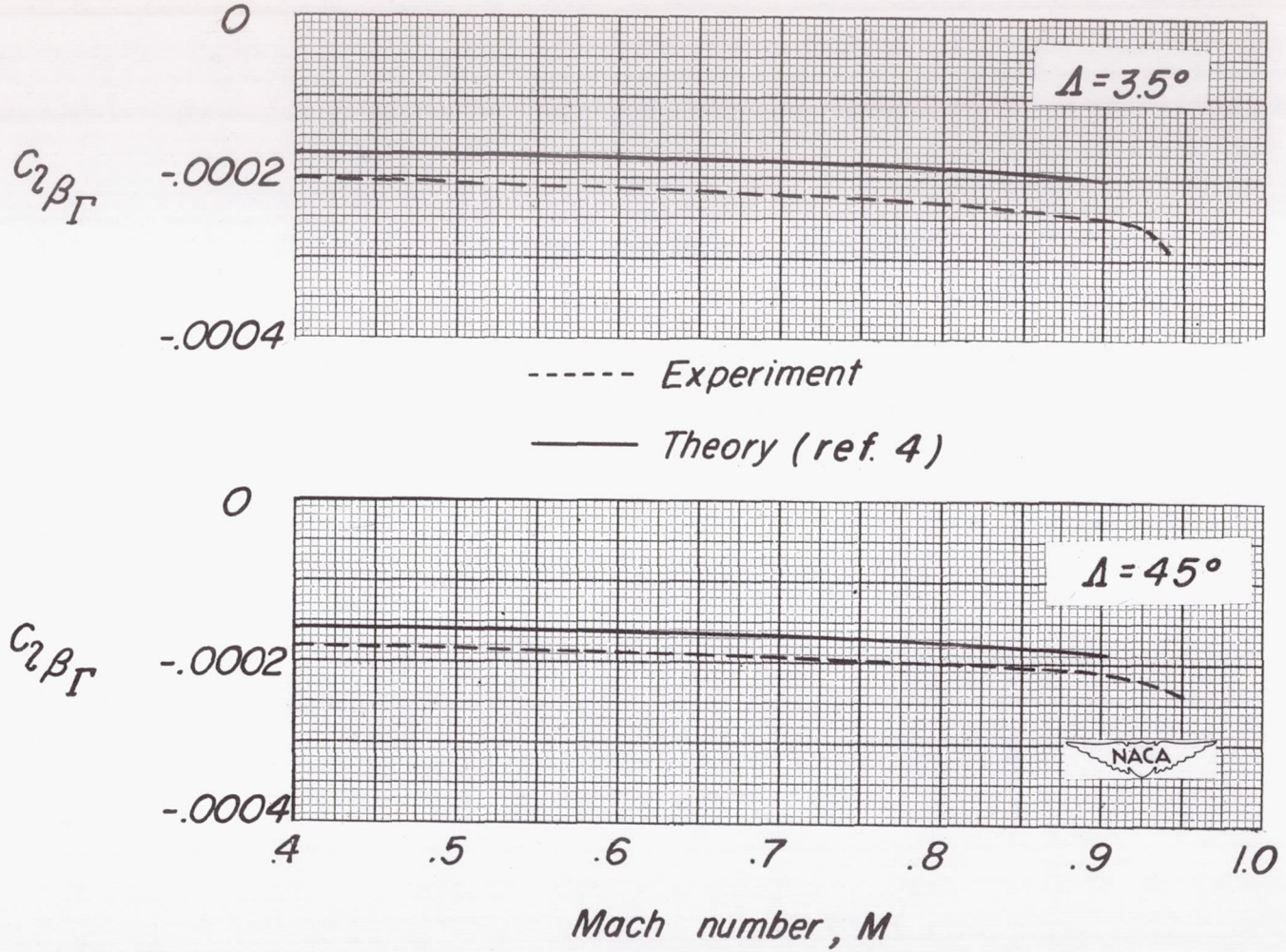

Figure 17.- Comparison of the theoretical and experimental variation of $C_{l_{\beta_\Gamma}}$ with Mach number. $\alpha = 0^\circ$.